LEVEL II

HDL-CR-80-100-1
April 1980

AD A084836

A Study of Fluidic Gun Stabilization Systems for Combat Vehicles: Final Report

by Charles L. Abbott
Thomas B. Tippett
Stephen M. Tenney
Charles Paras

DTIC
ELECTE
MAY 20 1980
C

Prepared by
AiResearch Manufacturing Co. of Arizona
111 South 34th Street
Phoenix, AZ 85010

Under contract
DAAG39-77-C-0100
DAAG39-78-C-0049

U.S. Army Electronics Research and Development Command
Harry Diamond Laboratories
Adelphi, MD 20783

Approved for public release; distribution unlimited.

DDC FILE COPY

80 5 16 052

The findings in this report are not to be construed as an official Department of the Army position unless so designated by other authorized documents.

Citation of manufacturers' or trade names does not constitute an official endorsement or approval of the use thereof.

Destroy this report when it is no longer needed. Do not return it to the originator.

PAGES _____

ARE

MISSING

IN

ORIGINAL

DOCUMENT

(2)

DTIC
ELECTE
MAY 2 0 1980
D

(9) FINAL REPORT. 6 Apr 77 - 30 Apr 79

(6) A STUDY OF FLUIDIC GUN STABILIZATION SYSTEMS FOR COMBAT VEHICLES, Revision B.

(14) 41-2374B (11) 28 Apr 80 (12) 86

(15) DAAG39-77-C-0100, DAAG39-78-C-0049

(18) HDL (19) CR-80-100-1

Supersedes AD-A080 [illegible]

(10) Charles L. Abbott Thomas B. Tippetts
Stephen M. Tennyson Charles Paras
Initial Issue
Approved by W. T. Flemington
L. I. Chambliss/Supvr., Documentation
Thomas B. Tippetts
Thomas B. Tippetts/Sr. Development Engineer
D. J. Schaffer
D. J. Schaffer/Sr. Project Engineer

AIRESEARCH MANUFACTURING COMPANY
A DIVISION OF THE GARRETT CORPORATION
PHOENIX, ARIZONA

404776

REPORT NO. 41-2304B

TOTAL PAGES 1

ATTACHMENTS: HDL-CR-80-100-1

REV	BY	APPROVED	DATE	PAGES AND/OR PARAGRAPHS AFFECTED
NC	OKI	TBT/DJS	6-28-79	Original Issue
A	OKI	TBT/DJS	2-15-80	Reference made to second draft issue of attached report.
B	OKI	TBT/DJS	4-28-80	Subject report revised to incorporate changes requested by HDL under Letter DELHD-R-CM-FS, dated March 6, 1980.

AIRESEARCH MANUFACTURING COMPANY OF ARIZONA
A DIVISION OF THE GARRETT CORPORATION
PHOENIX, ARIZONA

FINAL REPORT
A STUDY OF FLUIDIC GUN STABILIZATION SYSTEMS FOR COMBAT VEHICLES

41-2304B

DATE: April 28, 1980

The attached report is the final report for a study program conducted by AiResearch for the Department of the Army, Harry Diamond Laboratories, under Contracts DAAG39-77-C-0100 and DAAG-78-C-0049.

An AiResearch report number has been assigned to the report for record and retrieval purposes.

O. K. Isaacs
O. K. Isaacs
Engineering Sciences

Attachment: Report with above title

Accession For
NTIS GRA&I
DDC TAB
Unannounced
Justification
By
Distribution/
Availability Codes
Dist | Avail and/or special
A

UNCLASSIFIED

SECURITY CLASSIFICATION OF THIS PAGE (When Data Entered)

REPORT DOCUMENTATION PAGE	READ INSTRUCTIONS BEFORE COMPLETING FORM
1. REPORT NUMBER: HDL-CR-80-100-1	2. GOVT ACCESSION NO.: AD A084 836
3. RECIPIENT'S CATALOG NUMBER:	
4. TITLE (and Subtitle): A Study of Fluidic Gun Stabilization Systems For Combat Vehicles : Final Report	5. TYPE OF REPORT & PERIOD COVERED: Final Report for period 4-6-77 to 4-30-79
	6. PERFORMING ORG. REPORT NUMBER: 41-23043
7. AUTHOR(s): Charles L. Abbott, Stephen M. Tenney, Thomas B. Tippetts, Charles Paras	8. CONTRACT OR GRANT NUMBER(s): DAAG39-77-C-0100, DAAG39-78-C-0049
9. PERFORMING ORGANIZATION NAME AND ADDRESS: AiResearch Manufacturing Co. of Arizona, 111 South 34th Street, Phoenix, AZ 85010	10. PROGRAM ELEMENT, PROJECT, TASK AREA & WORK UNIT NUMBERS:
11. CONTROLLING OFFICE NAME AND ADDRESS: Harry Diamond Laboratories, 2800 Powder Mill Road, Adelphi, MD 20783	12. REPORT DATE: April 1980
	13. NUMBER OF PAGES: 81
14. MONITORING AGENCY NAME & ADDRESS(if different from Controlling Office)	15. SECURITY CLASS. (of this report): Unclassified
	15a. DECLASSIFICATION/DOWNGRADING SCHEDULE:

16. DISTRIBUTION STATEMENT (of this Report)

Approved for public release; distribution unlimited.

17. DISTRIBUTION STATEMENT (of the abstract entered in Block 20, if different from Report)

18. SUPPLEMENTARY NOTES

HDL Projects: 304834, 356834
DRCMS Code: 8-612603.H1.80011.GG-GG
PRON: A18R010701A1A9, 1A825538GGA9

19. KEY WORDS (Continue on reverse side if necessary and identify by block number)

Gun stabilization system
Fluidic control system
Fluidic angular rate sensor
Fluidic amplifiers

20. ABSTRACT (Continue on reverse side if necessary and identify by block number)

A control system was developed for stabilization of the main gun of an armored combat vehicle. The system maintains target alignment of the gun while the vehicle is maneuvering over uneven terrain. The system utilizes fluidic technology for motion sensing, computation, and servovalve control. The program encompassed system dynamic analysis, laboratory testing, and on-vehicle development.

DD FORM 1 JAN 73 1473 EDITION OF 1 NOV 65 IS OBSOLETE

UNCLASSIFIED

SECURITY CLASSIFICATION OF THIS PAGE (When Data Entered)

FOREWORD

This is the final report of a program conducted by AiResearch Manufacturing Company of Arizona, a Division of The Garrett Corporation. The purpose of the program was to study, define, design, fabricate, and test a two-axis gun stabilization system using fluidic technology. Work performed under the present contract constitutes the fourth year of effort on a program sponsored by the U.S. Army Harry Diamond Laboratories (HDL) to demonstrate the reliability, ruggedness, and cost advantages of fluidic technology in components of a gun stabilization system.

The primary objective of the present contract was to design and fabricate a two-axis system capable of meeting or exceeding the performance requirements of the electrohydraulic add-on stabilization system now used on the M60A1 tank. The system was installed, tested, and demonstrated in an M48A5 tank at the AiResearch test laboratory in Phoenix, Arizona.

The program was authorized by the Department of the Army under Contracts DAAG39-77-C-0100 and DAAG39-78-C-0049 and was conducted from April 6, 1977, to April 30, 1979, under AiResearch Master Work Orders 3409-248128-01-0X00 and 3409-248126-01-0X00.

Technical direction and support were provided by Mr. J. Joyce (Program Monitor) of HDL. Technical support was provided also by Mr. Jack Connors of the Weapon System Branch, Armament Research and Development Command.

CONTENTS

FIGURES

CONTENTS (Contd)

TABLES

1. INTRODUCTION

The system described in this report is intended for installation in combat vehicles such as tanks and armored personnel carriers, for the purpose of assisting the gunner in maintaining accurate gun alignment with the selected target while the gun mounting is being subjected to random disturbances caused by vehicle motion over uneven terrain. The system uses fluidic angular rate sensors and amplifiers operating with air as the fluid medium to sense angular rate, perform dynamic compensation, and operate servovalves to reposition the gun and turret to maintain target alignment. A dynamic analysis of the system is presented. Components were designed, fabricated, tested, and assembled into a system which was installed and tested on an M48A5 tank.

2. SYSTEM DEFINITION

2.1 General Description

The system developed was designed to sense gun motion, amplify and dynamically compensate the signal, and operate valves which reposition the turret and gun actuators to keep the gun aligned with the target. The controllers for the elevation and traverse axes, while similar in concept, are designed differently to accommodate differences in the dynamic performance between the elevation and traverse actuation systems. Block diagrams of the traverse- and elevation-axis systems are shown in Figures 1 and 2, and schematic diagrams of the fluidic controllers are shown in Figures 3 and 4.

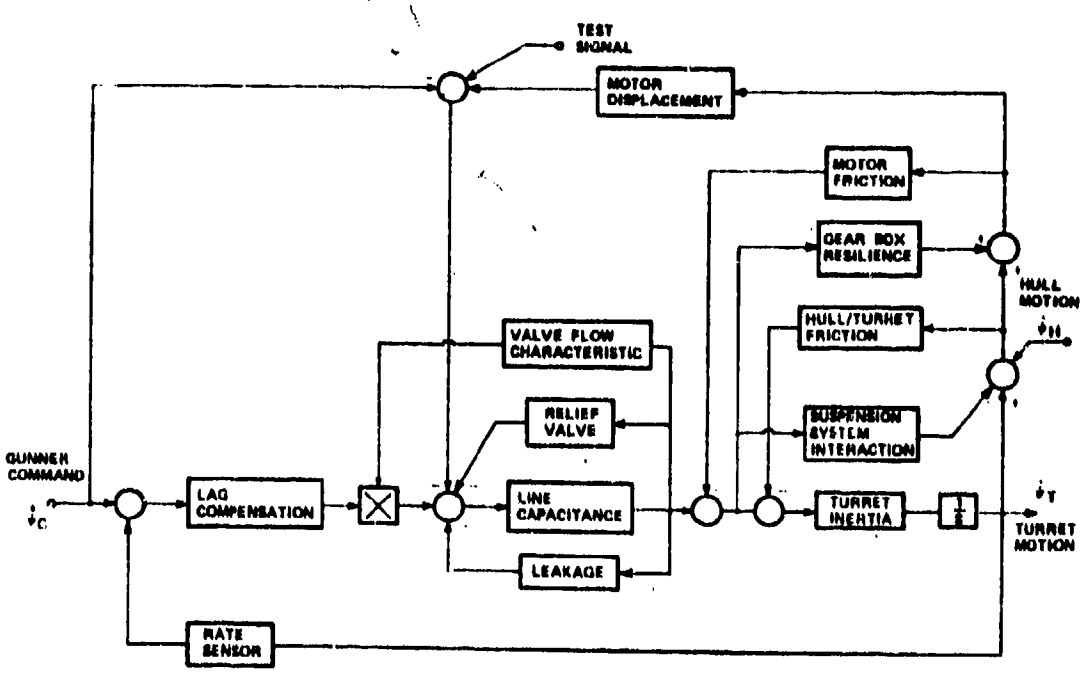

Figure 1. General block diagram of traverse-axis controller system.

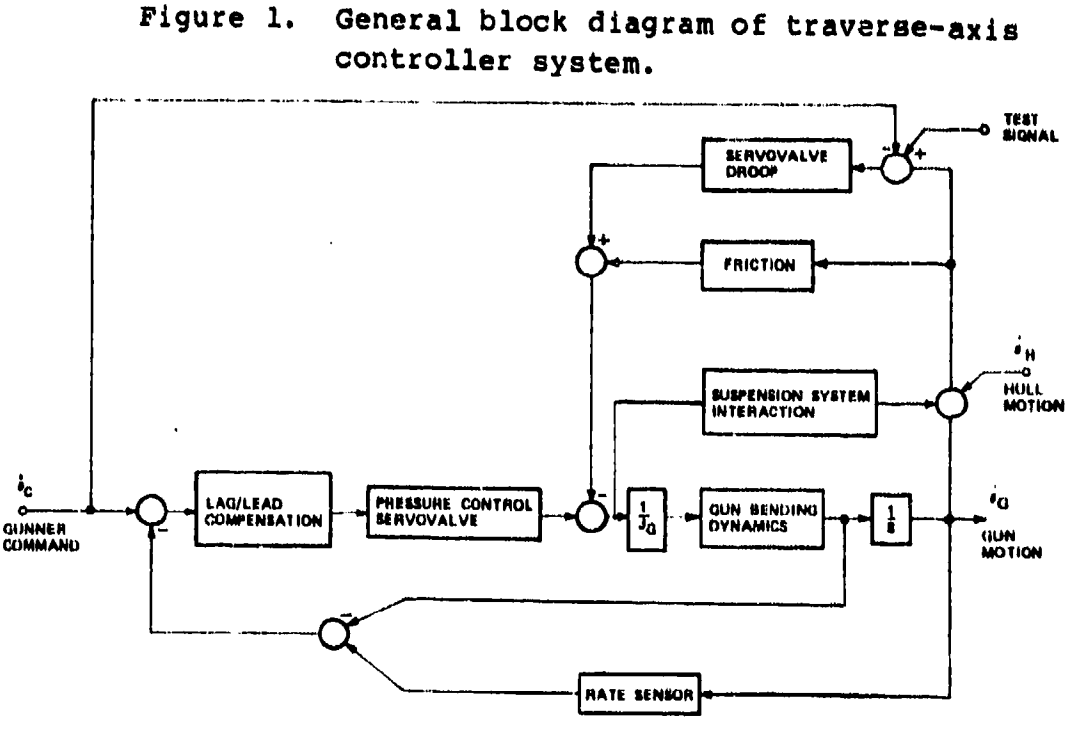

Figure 2. General block diagram of elevation controller system.

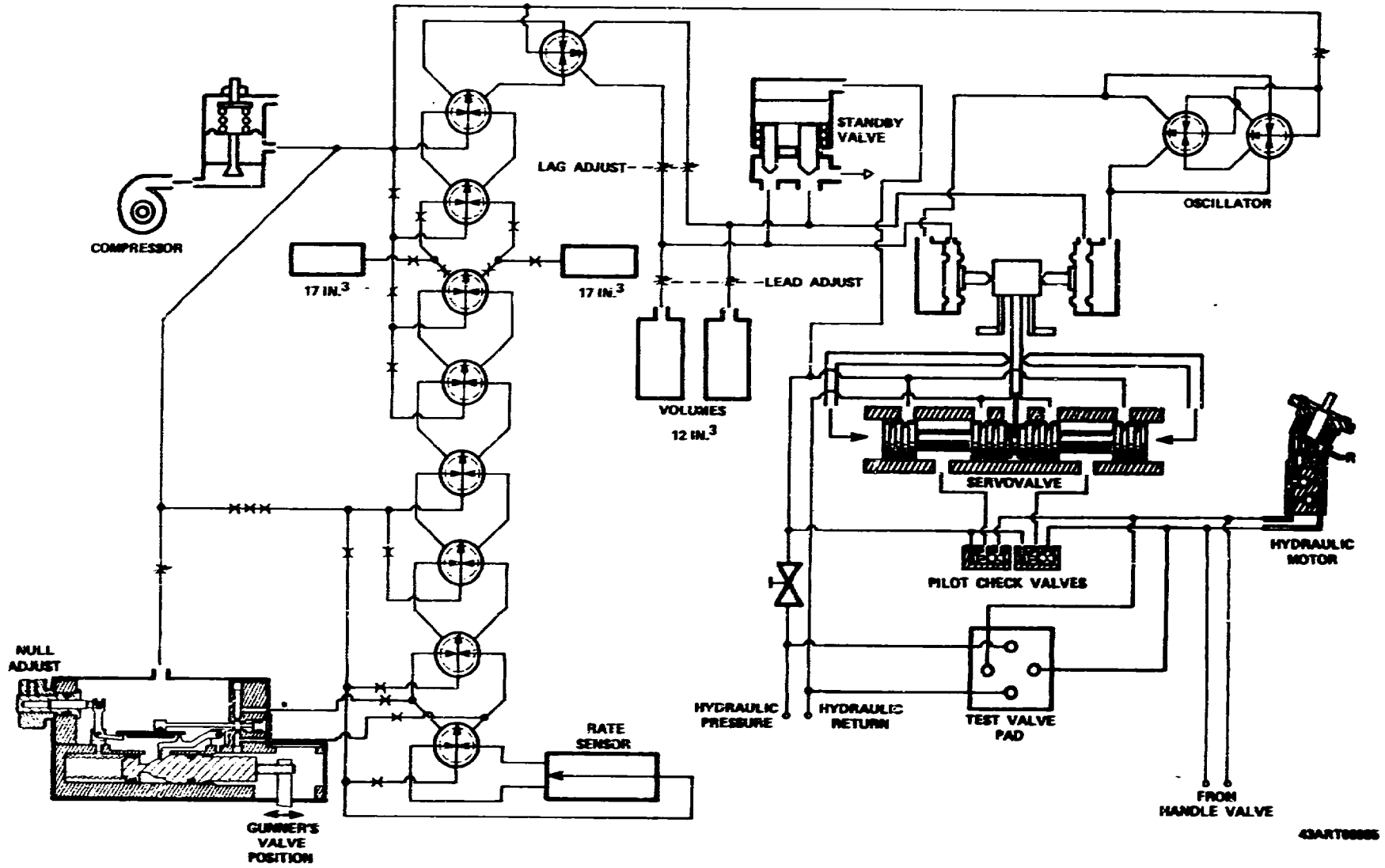

Figure 3. Schematic diagram of transverse controller system.

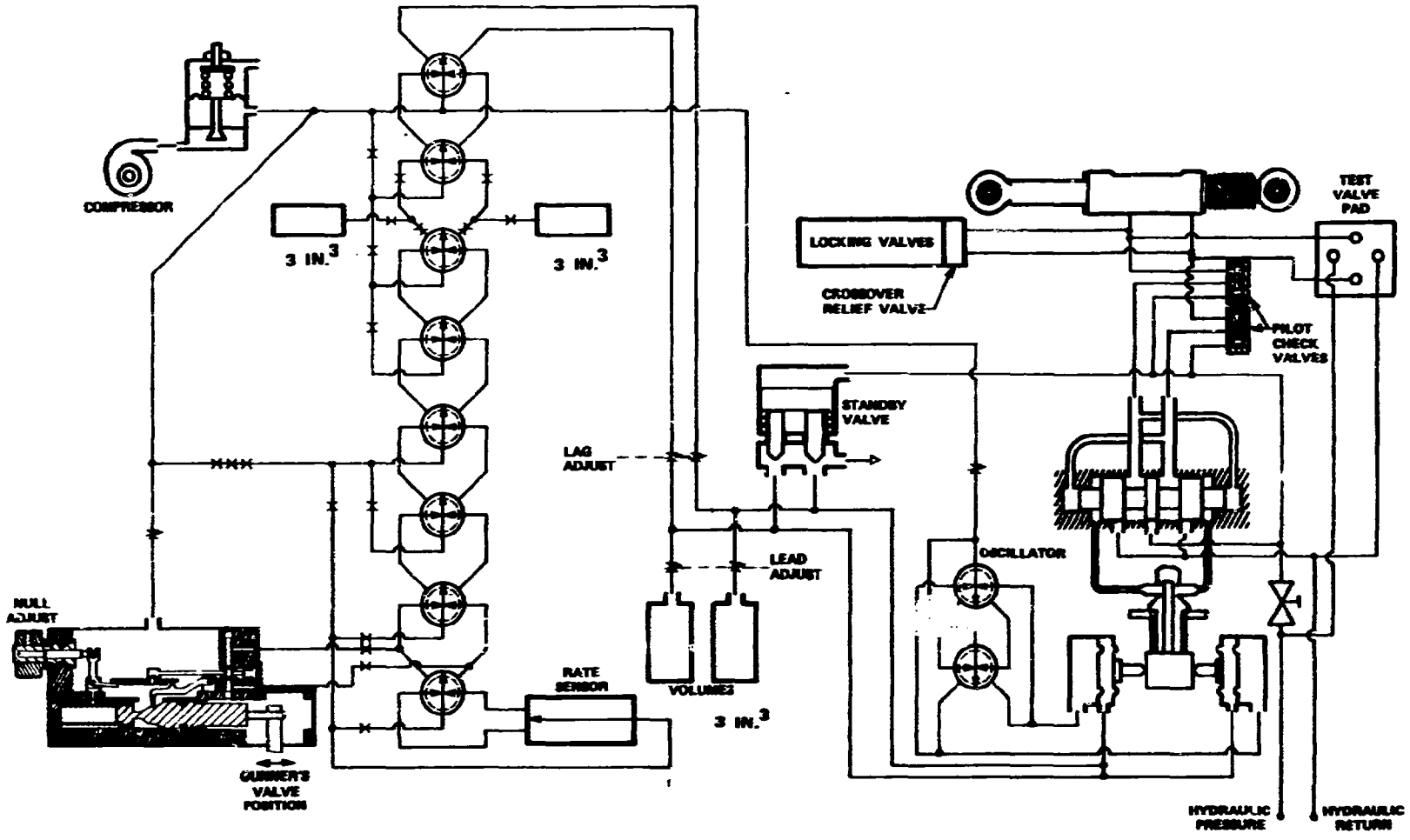

Figure 4. Schematic diagram of elevation controller system.

Rate sensing is performed by a laminar jet angular rate sensor (LJARS), a device developed at the Harry Diamond Laboratories. This device, shown schematically in Figure 5 and detailed in Appendix A, senses angular rate by measuring the Coriolis-induced curvature in a jet issuing from a nozzle when the nozzle is rotated.

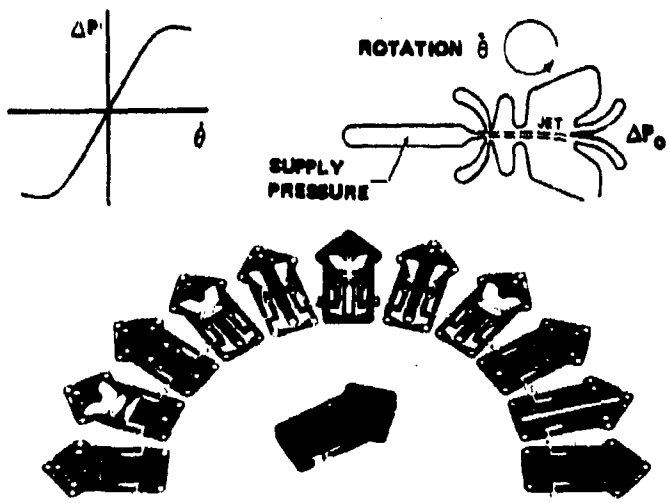

Figure 5. Fluidic angular rate sensor.

The rate sensor output is amplified and compared to the pressure signal representing the commanded rate from the gunner. The commanded rate signal is obtained by a gunner's handle position sensor which is mechanically linked to the gunner's handle valve. As the gunner commands a rate, the valve motion produces an offset in a pneumatic flapper valve. The resulting error signal is dynamically compensated by a resistor-volume combination which performs a lag or a lag-lead function. The compensated error signal is then applied to the servovalve which controls flow to the actuator or motor.

The servovalve in the elevation axis controller contains pressure feedback. A pressure control valve is dynamically suited to suppressing the high frequency disturbances encountered in the elevation axis.

The servovalve contained in the traverse axis controller is a flow rate control valve. Flow rate control in the traverse axis is desirable to obtain smooth, constant rate target tracking performance. Flow rate control is mechanized by spool position feedback using a flapper nozzle actuated by the spool.

The fluidic stabilization system is contained primarily in three packages illustrated in Figure 6: (1) a traverse (azimuth) controller which is located on the turret wall in the position presently occupied by the electrohydraulic stabilization system servovalve assembly; (2) the elevation controller which is installed in the position on the gun presently occupied by the electrohydraulic stabilization system manifold and servovalve assembly; and (3) a gunner's handle position sensor assembly located on top of the gunner's handle valve assembly, replacing the cover and the arms used to sense the position of the gunner's hydraulic power valves in the electrohydraulic stabilization system. Also illustrated are three of the components used from the electrohydraulic stabilization system.

2.2 Dynamic Analysis

Dynamic performance of the system was predicted using a linear frequency response model derived from experimental measurements. (Refer to simplified block diagrams in Figures 7 and 8.) Transfer functions for the turret drive and gun actuation systems were obtained by measuring gun and turret motion with a rate gyroscope while the turret drive motor and gun actuator were being excited sinusoidally by servovalves driven by a signal generator. Data obtained from these tests are plotted in Figures 9 and 10 for the azimuth and elevation axis, respectively. Curve fit equations are also plotted in Figures 9 and 10.

The azimuth transfer function was approximated by the following curve fit equation.

$$G_T = \frac{\psi_T}{\psi_V} = \frac{\dfrac{S^2}{\omega_H^2} + \dfrac{2\zeta_H S}{\omega_H} + 1}{\left(\dfrac{S^2}{\omega_T^2} + \dfrac{2\zeta_T S}{\omega_T} + 1\right)\left(\dfrac{S^2}{\omega_H^2} + \dfrac{2\zeta_H S}{\omega_H} + 1\right) + \left(\dfrac{J_T}{J_H}\dfrac{S^2}{\omega_H^2}\right)\left(\dfrac{2\zeta_T}{\omega_T^2} + 1\right)}$$

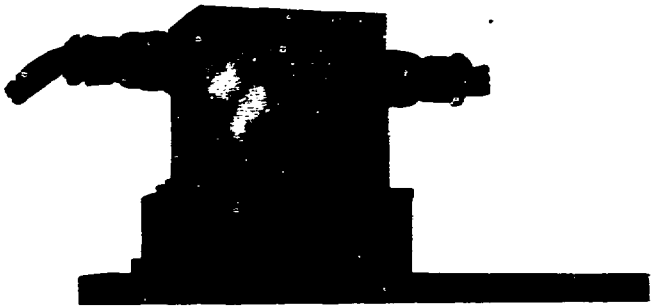

HANDLE CONTROL ASSEMBLY

HYDRAULIC SHUTOFF VALVE

ANTIBACKLASH CYLINDER

FILTER

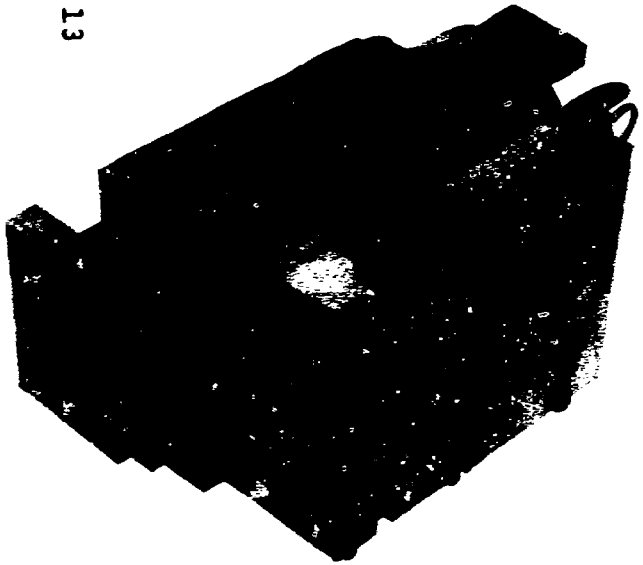

ELEVATION CONTROLLER ASSEMBLY

AZIMUTH CONTROLLER ASSEMBLY

Figure 6. Fluidic gun stabilization system components. P-67696-1

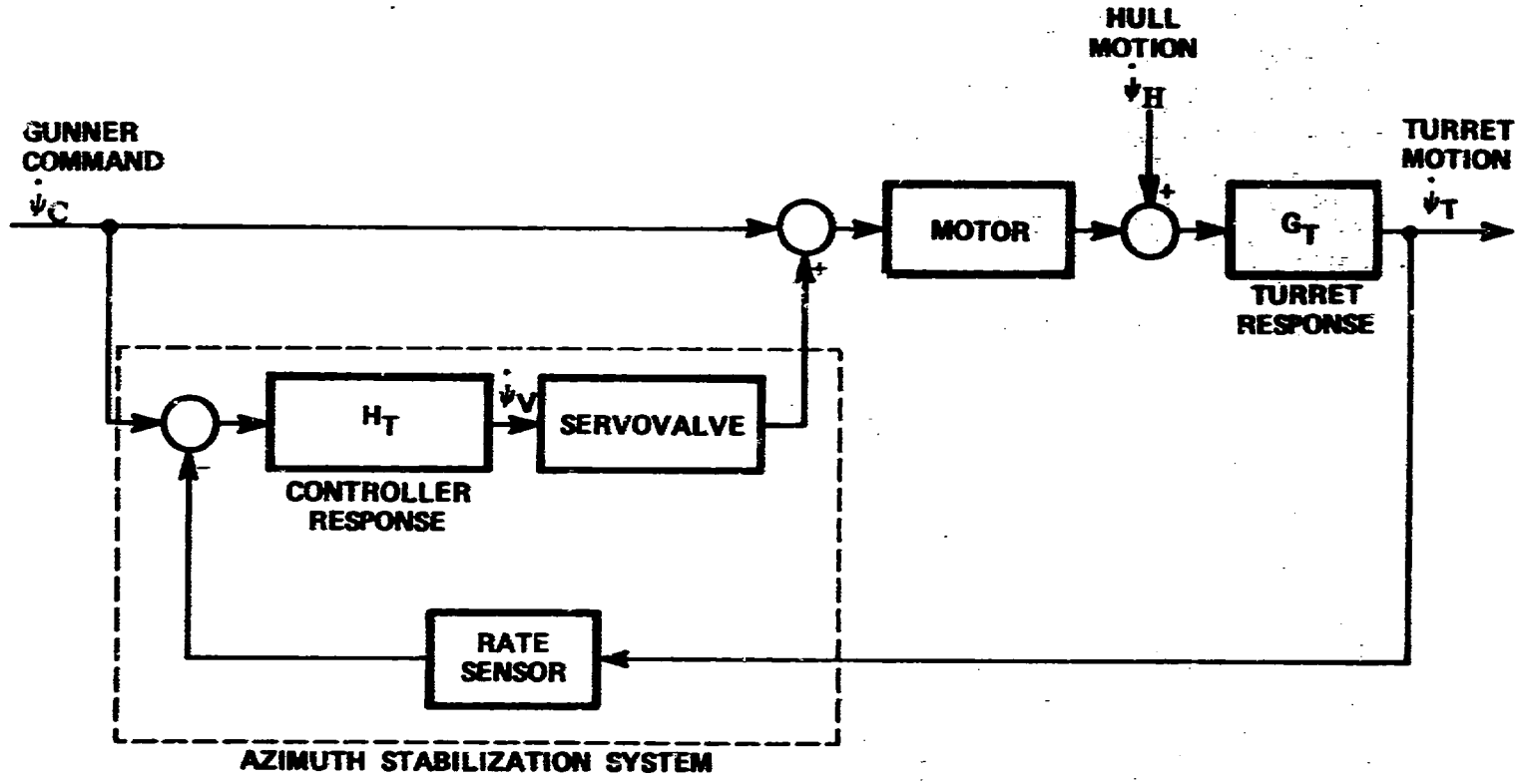

Figure 7. Simplified block diagram of azimuth system.

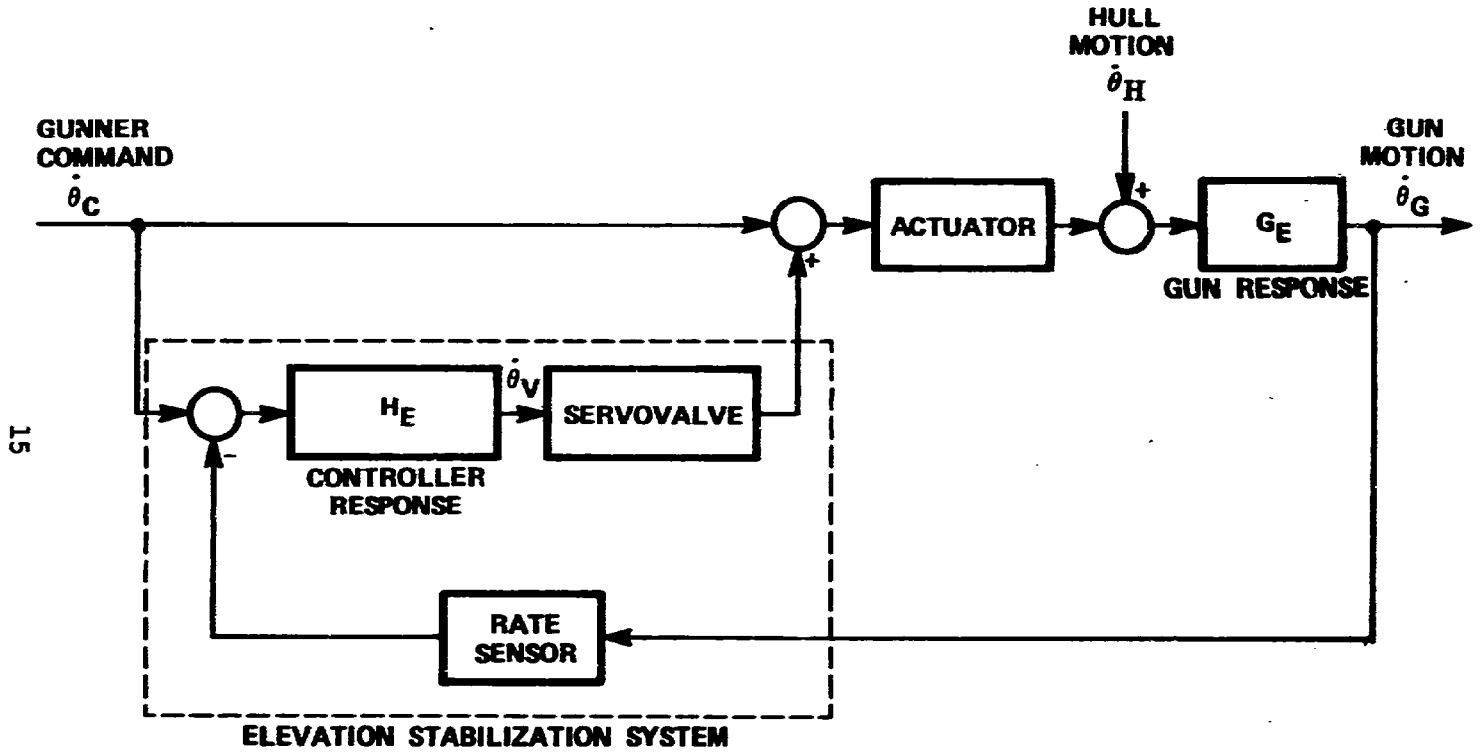

Figure 8. Simplified block diagram of elevation system.

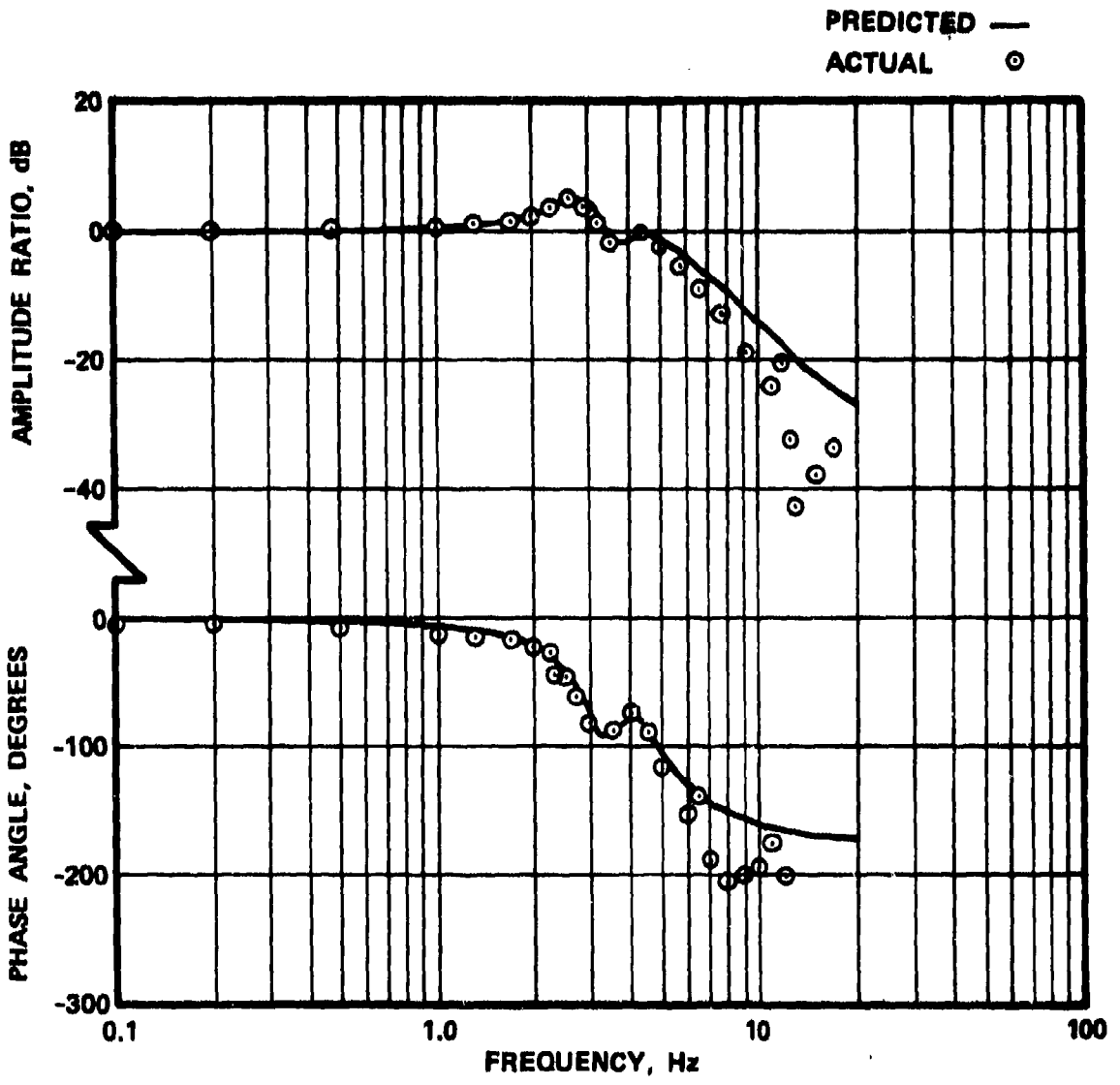

Figure 9. Turret actuation system response.

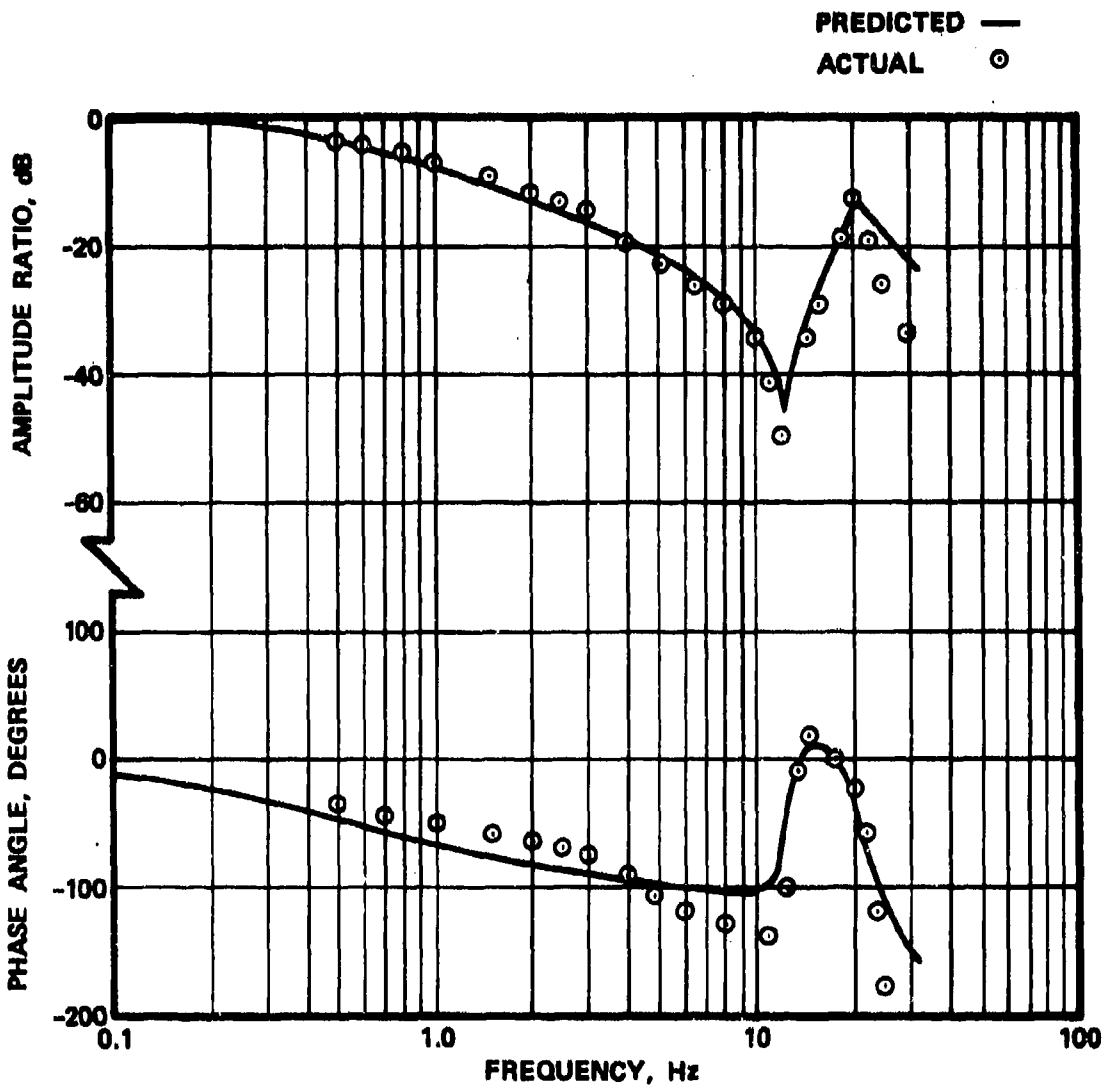

Figure 10. Gun elevation actuation system response.

where

$\dot{\psi}_T$ = angular velocity of turret (rad/s),

$\dot{\psi}_V$ = angular velocity command to servovalve (rad/s),

S = Laplace transform variable (rad/s),

ω_H = hull suspension natural frequency in azimuth axis,

= 22 rad/s,

ζ_H = hull suspension damping ratio,

= 0.15,

ω_T = turret drive natural frequency,

= 26 rad/s,

ζ_T = turret drive damping ratio,

= 0.030,

J_T = turret moment of inertia,

= 3143 kg-m-s^2,

J_H = hull moment of inertia

= 18,435 kg-m-s^2.

The elevation actuation system transfer function was approximated by

$$G_E = \frac{\dot{\theta}_G}{\dot{\theta}_V} = \left[\frac{1}{1 + \tau_G S} + \frac{KS}{\frac{S^2}{\omega_G^2} + \frac{2\zeta_G S}{\omega_G} + 1} \right] e^{-\tau_e S}$$

where

$\dot{\theta}_G$ = angular rate of gun in elevation axis (rad/s),

$\dot{\theta}_V$ = angular rate command to servovalve (rad/s),

τ_G = servovalve droop time constant,

= 0.318 s,

K = 3.33×10^{-4} s

ω_G = gun barrel resonant frequency,

= 131.9 rad/s,

ζ_G = gun barrel damping ratio,

= 0.10,

τ_e = empirical transport delay,

= 0.007 s.

2.3 Controller Performance Specification

Closed loop performance of the azimuth system is calculated by the function

$$\frac{\dot{\psi}_T}{\dot{\psi}_H} = \frac{G_T}{1 + G_T H_T}$$

where H_T is the transfer function of the azimuth controller and is shaped to obtain optimum closed loop dynamic response. Nearly optimum performance is achieved when

$$H_T = K_L \frac{(1 + \tau_1 S)(1 + \tau_2 S)}{(1 + \tau_3 S)(1 + \tau_4 S)} \frac{e^{-\tau_r S}}{1 + \tau_5 S}$$

where

K_L = 100, specified system loop gain,

τ_1 = 0.05 s, τ_2 = 0.28 s } dynamic compensation lead time constants,

τ_3 = 2.54 s, τ_4 = 1.60 s } dynamic compensation lag time constants,

τ_5 = 0.008 s, response time constant of servovalve input diaphragms and associated pneumatic ducting,

τ_r = 0.005 s, transport delay time associated with rate sensor and fluidic amplifier.

Predicted closed loop response of turret motion to hull motion is plotted in Figure 11.

Closed loop performance of the elevation system is calculated by the next equation.

$$\frac{\dot{\theta}_G}{\dot{\theta}_H} = \frac{G_E}{1 + G_E H_E}$$

Nearly optimum performance is obtained when

$$H_E = K_L \frac{(1 + \tau_6 S)}{(1 + \tau_8 S)} \frac{(1 + \tau_7 S)}{(1 + \tau_9 S)} \frac{e^{-\tau_r S}}{(1 + \tau_5 S)}$$

where

$\tau_6 = \tau_7$ = 0.133 s, dynamic compensation lead time constants,

$\tau_8 = \tau_9$ = 0.396 s, dynamic compensation lag time constants.

Predicted closed loop response of gun motion to hull motion is plotted in Figure 12.

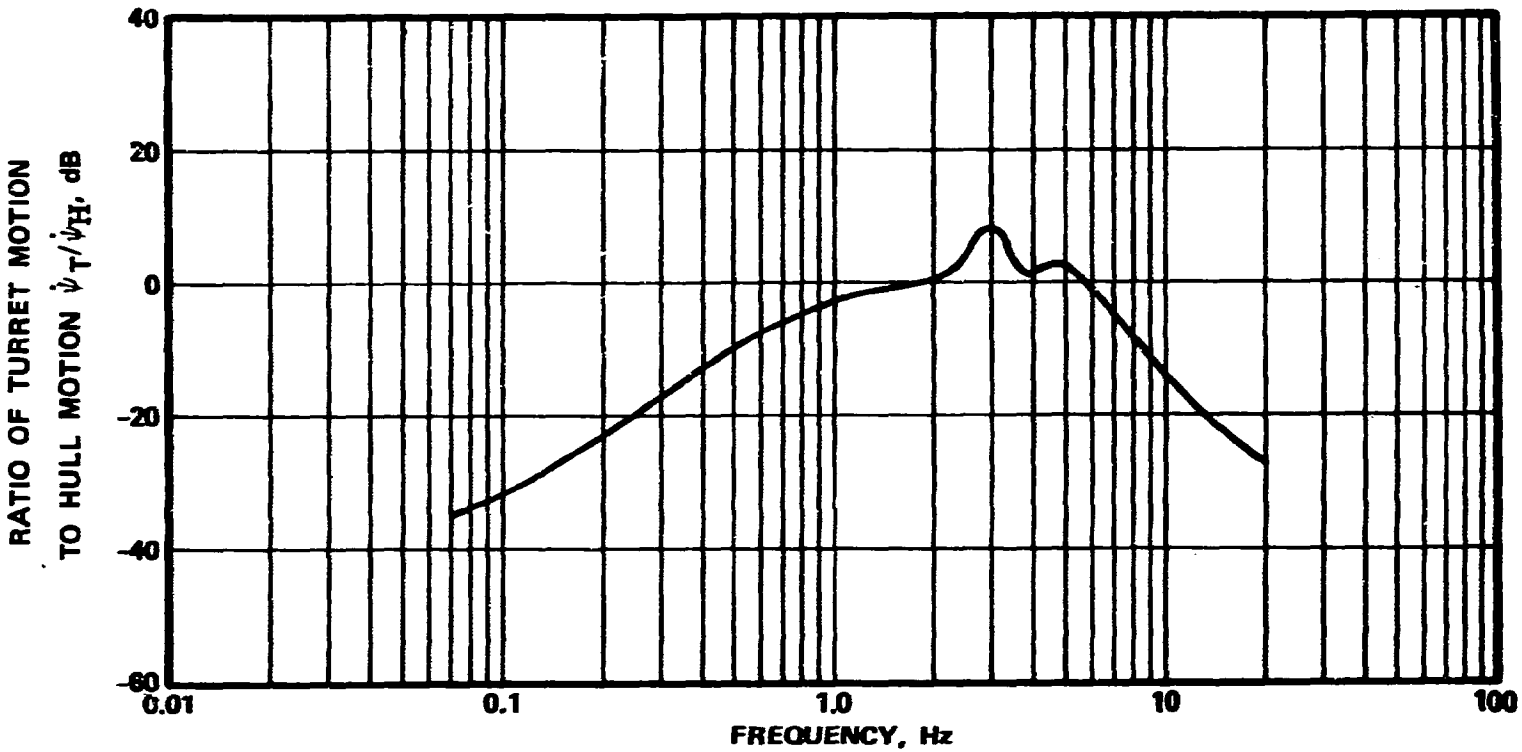

Figure 11. Predicted closed loop response of azimuth system.

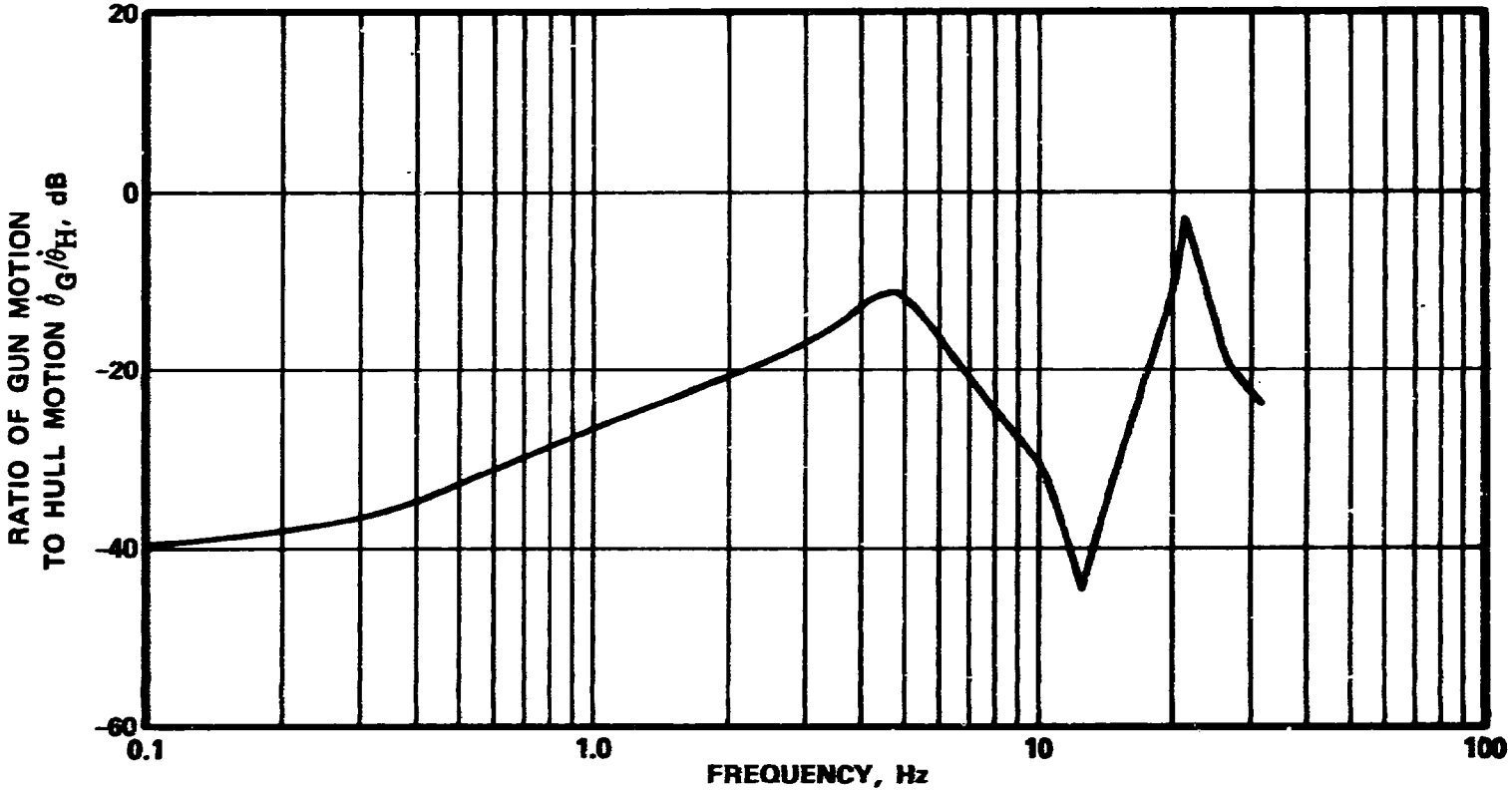

Figure 12. Predicted closed loop response of elevation system.

2.4 Hardware Design

Hardware designed for this program is contained in three packages. The elevation axis package occupies the space presently occupied by the electrohydraulic system servovalve and associated manifold and mounts directly to the actuator. The azimuth axis package occupies the space under the ballistic computer presently utilized by the electrohydraulic system azimuth servovalve and manifold. The gunner's handle position sensor replaces the cover on the gunner's handle valve assembly and is linked to the gunner's power valves. Several components provided with the electrohydraulic system were utilized in the fluidic system. Among these are the stabilization solenoid valve, antibacklash mechanism, pilot check valves, and filter.

Both controllers were constructed around a concept that used a machined housing on which the laminated manifolds were mounted and which provided interconnections between manifolds.

The components, in turn, were mounted on the laminated manifolds which provide the interconnections between components. Major components mounted in this manner are the laminated rate sensors and fluidic amplifiers, servovalves, and air compressors.

The fluidic rate sensor and amplifiers operate on air which is supplied by a compressor at approximately 10 psi. The pneumatic-hydraulic interface is made with modified servovalves of the same type used in the electrohydraulic system.

Photographs of the azimuth and elevation controllers and the handle pickoff assembly in their installed positions are presented in Figures 13, 14, and 15.

3. COMPONENT DEVELOPMENT

3.1 Rate Sensor Development

The laminar jet rate sensor required several refinements in design and method of manufacture to meet the accuracy requirements of a gun stabilization system. Errors are introduced by offset and gain shifts when rate sensor supply pressure and fluid temperature (i.e., viscosity) vary.

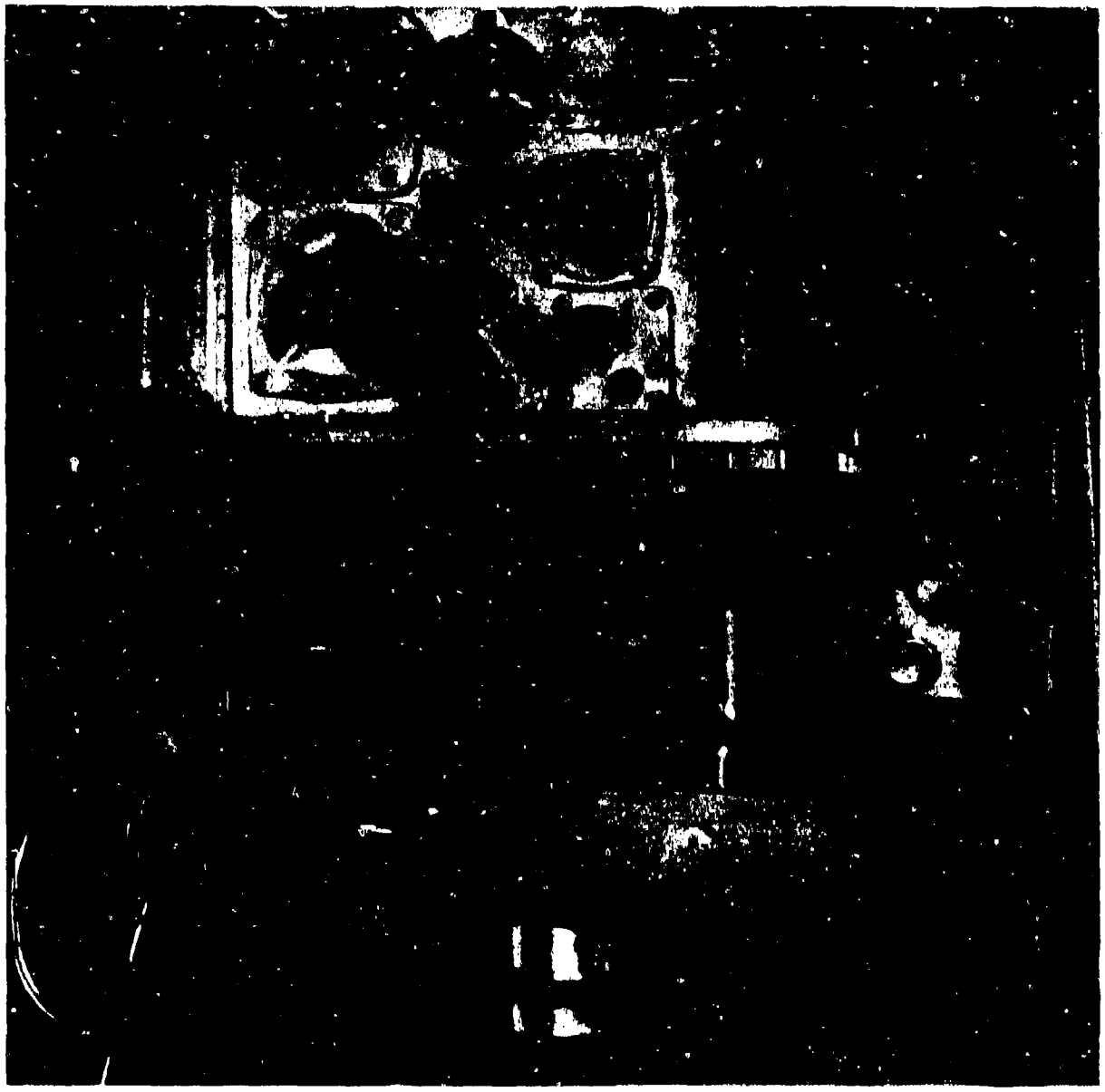

P-64181-2

Figure 13. Installed azimuth controller.

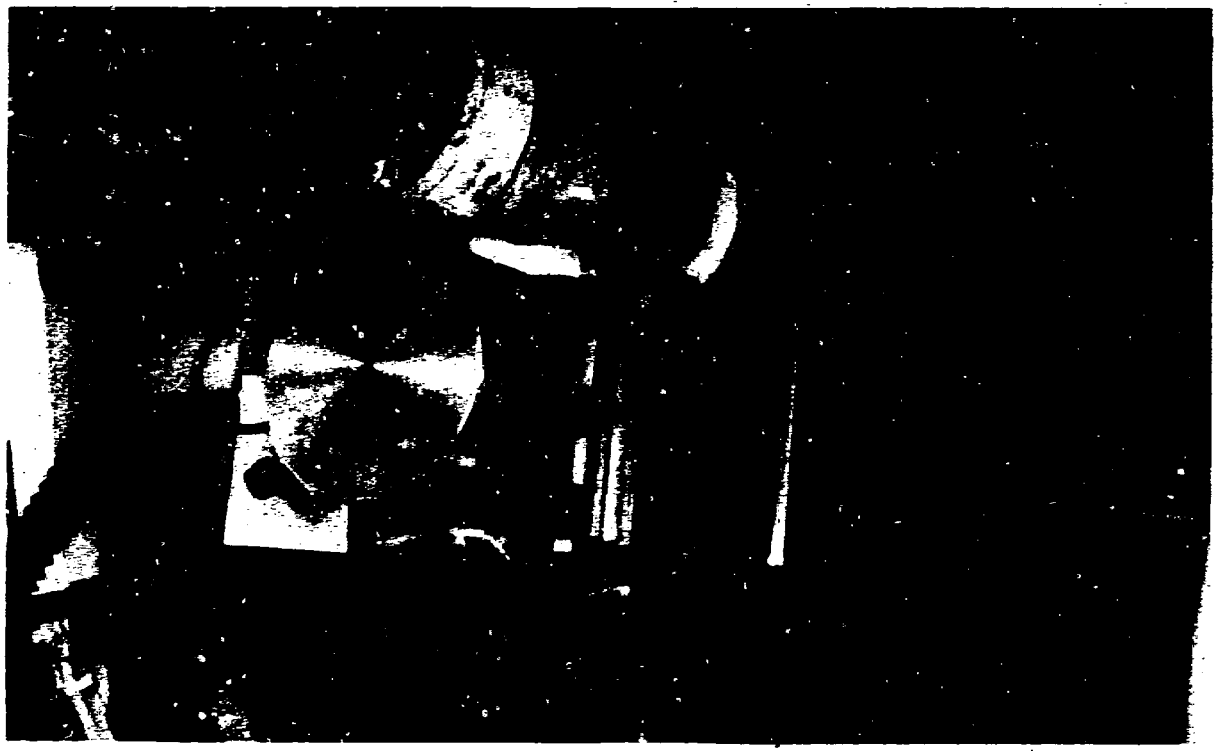

P-64181-1

Figure 14. Installed elevation controller.

Figure 15. Installed gunner's handle position sensor. P-67696-2

The effect of gain shift on system performance is to change system damping and suppression ratios. No attempt was made to reduce or compensate for sensor gain variations because damping and suppression ratio changes were not significant over the limited environmental conditions encountered during testing. Gain compensation could be applied to this system during future development to accommodate more severe environmental conditions.

The effect of offset shift, however, was more pronounced because sensor offset appears as drift that must be removed periodically by repositioning the gunner's null adjustment knob. Too frequent readjustment is objectionable and reduces the gunner's ability to hold and track the target.

Offset shifts resulting from pressure and temperature variations occur primarily because of manufacturing inaccuracies and asymmetries in rate sensor splitter, supply nozzle, and output channels. As noted in Figure 16, the effect of splitter asymmetry (i.e., the splitter not located on the jet center line) is an offset in output pressure, ΔP_o, that increases or decreases monotonically with Reynolds number, N_R. Offsets due to splitter asymmetry were removed by providing an adjustment that moves the splitter to the jet center line by bending the sensor body.

The effect of asymmetry in nozzle exit geometry is a bending of the jet as it leaves the nozzle (see Figure 17). The bending angle, α, is sensitive to Reynolds number because the flow separation points move differently as Reynolds number is increased or decreased. The result is a nonmonotonic output pressure offset that can be removed by the splitter adjustment at only one value of Reynolds number. Variations in Reynolds number about that one value cause positive or negative offsets in output pressure. By providing an adjustment that enables the sides of the nozzle to be moved relative to each other and parallel to the nozzle center line, a relative position can be found where the flow separation points will remain in reasonably symmetrical correspondence with each other as Reynolds number is varied over some range. Jet bending angle and therefore offset pressure, ΔP_o, will remain constant over this range of Reynolds number.

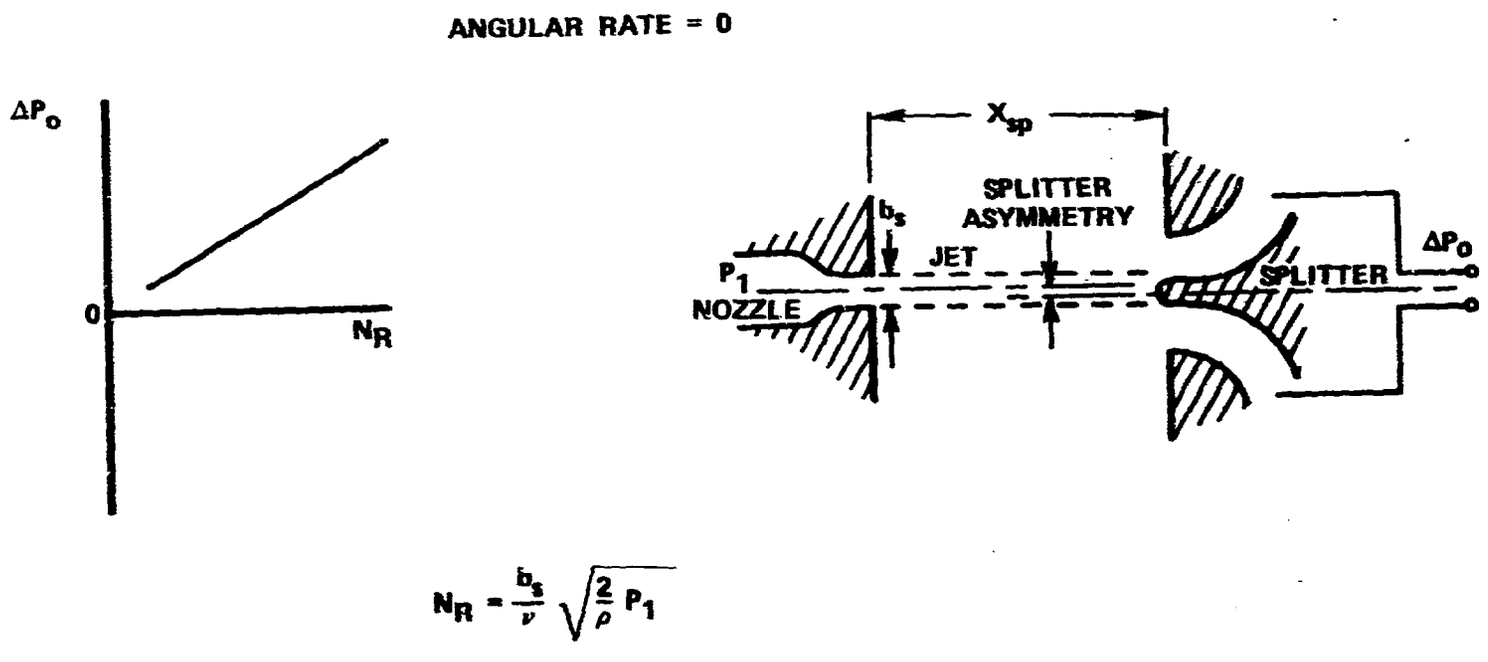

$$N_R = \frac{b_s}{\nu}\sqrt{\frac{2}{\rho}P_1}$$

Figure 16. Effect of splitter asymmetry on rate sensor offset.

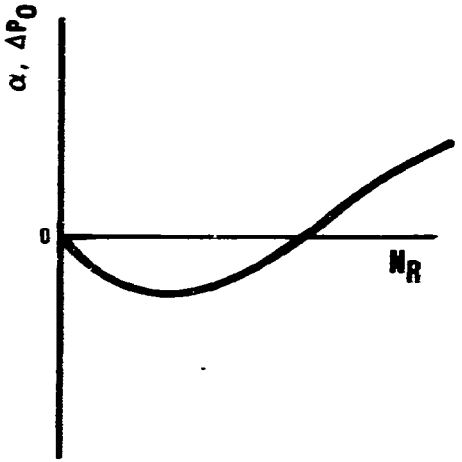

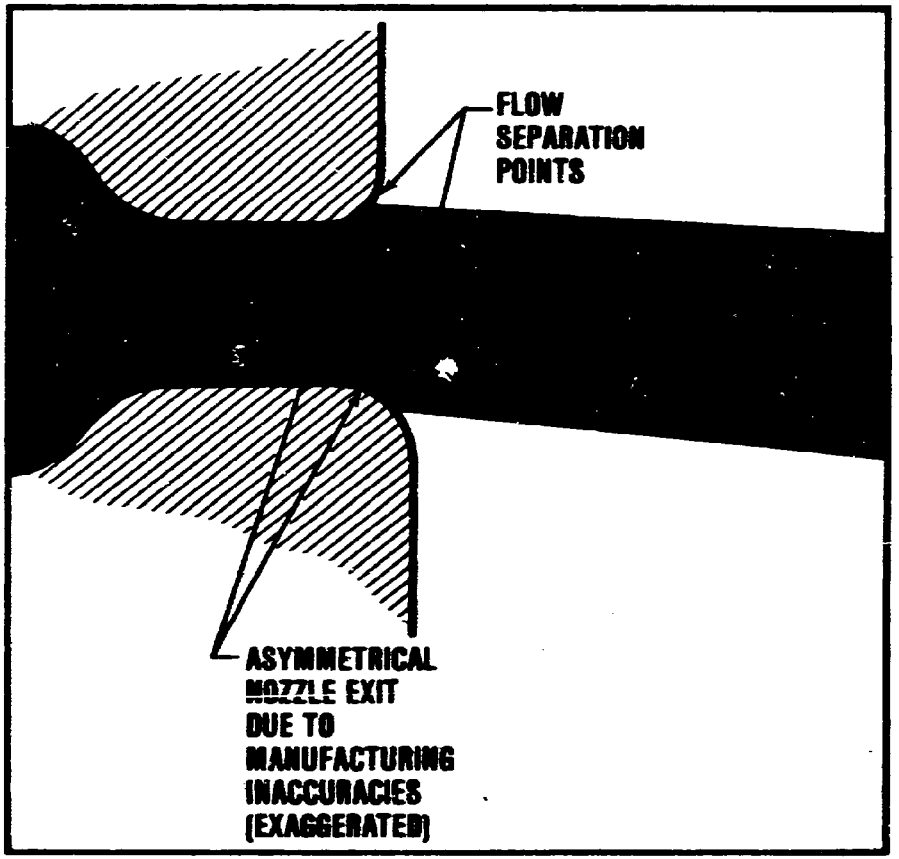

Figure 17. Effect of nozzle exit asymmetry on rate sensor offset.

By alternately manipulating the splitter symmetry adjustment and the nozzle symmetry adjustment, a setting can be found where offset pressure, ΔP_o, will remain near zero over a Reynolds number range sufficient to accommodate expected variations in supply pressure and temperature.

The Reynolds number range over which ΔP_o remains near zero increases as variations in geometry due to manufacturing tolerances are decreased. The rate sensor hardware used in this program was fabricated by numerically controlled wire electrical discharge machining (wire EDM) process. This process provided the best accuracy obtainable from the manufacturing methods that were reasonably available.

Figure 18 exhibits data showing the reduction in offset variation obtained by manipulating the splitter and nozzle symmetry adjustments. Rate sensor sensitivity is plotted in Figure 19.

Another source of offset variation with changes in Reynolds number is asymmetry in the length and the width of the output channels. An early rate sensor model was purposely designed with unequal output channels to accommodate a more efficient installation position. Offset variation was reduced by a subsequent rate sensor redesign that incorporated symmetrical output channels.

3.2 Fluidic Amplifiers

To amplify the low level rate sensor signal to a value suitable for actuating the system servovalve, nine stages of fluidic amplification were used. This amplifier cascade yielded a steady-state gain of approximately 3×10^6. Laminar proportional amplifiers (detailed in Appendix A) were used for the first seven stages because of their quiet, high gain performance. The output stages were turbulent centervent amplifiers which were well suited for driving a blocked load such as the servovalve input. For each stage of amplification, the amplifier size and supply pressure used are shown in Table I. Detailed stacking orders of laminates used to assemble the gain blocks for each control axis are presented in Appendix B.

3.3 Air Compressor

Each of the two controllers contain identical pneumatic power supplies. They consist of a motor-compressor assembly, electronic speed control, and pressure regulator.

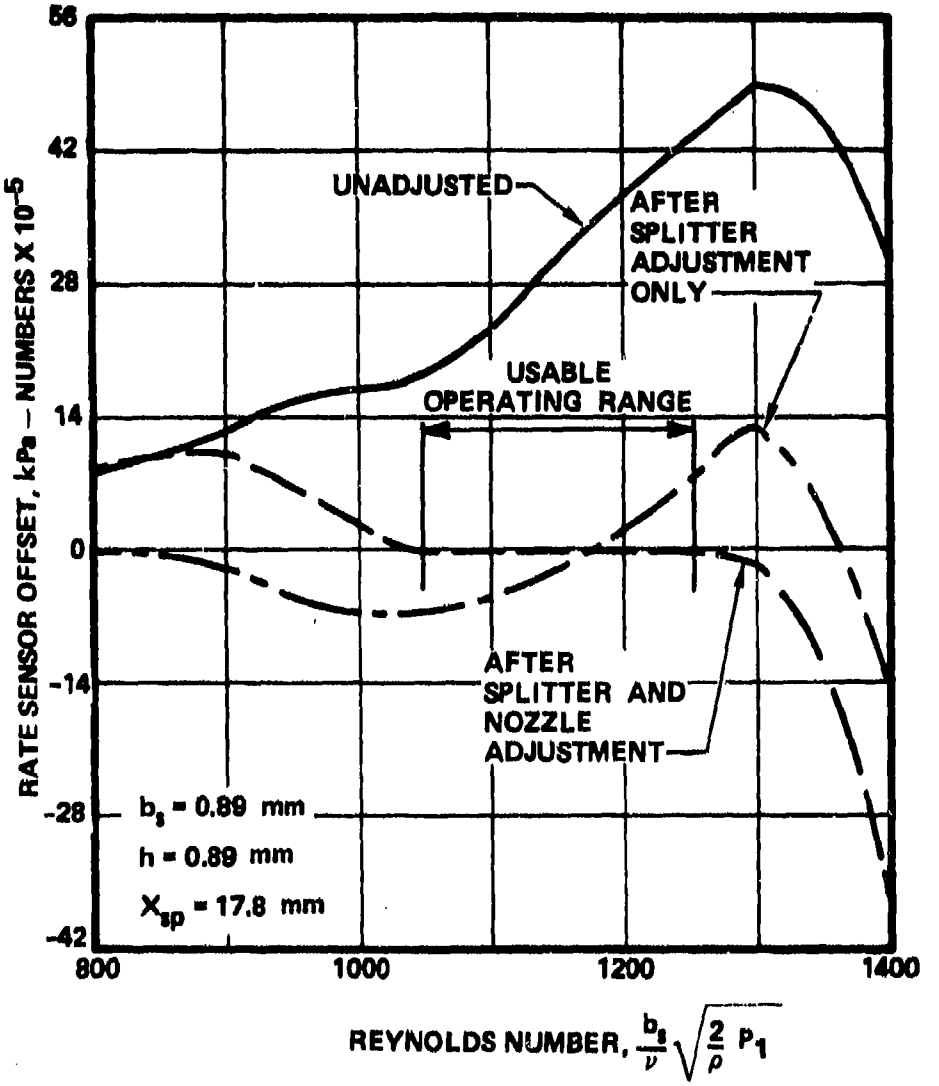

Figure 18. Effect of rate sensor adjustments.

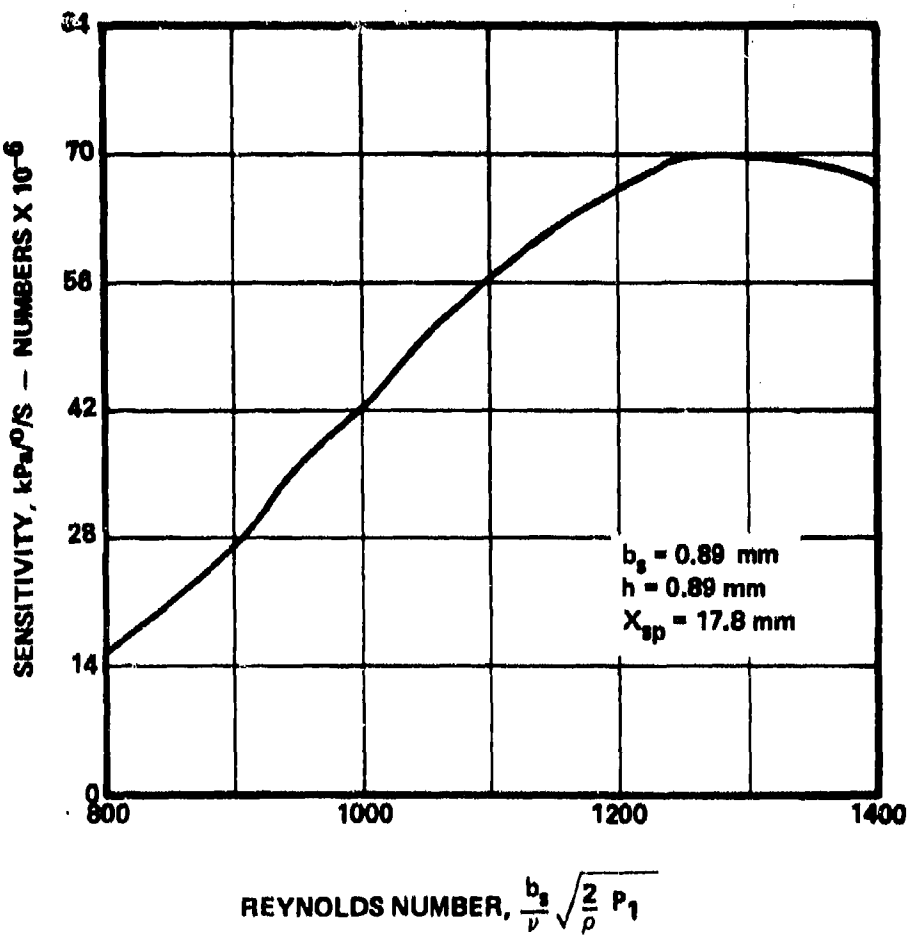

Figure 19. Rate sensor sensitivity.

TABLE I. AMPLIFIERS IN FLUIDIC GAIN BLOCK

Stage	bs (mm)	h (mm)	Ps (kPa)
1	0.76	0.76	0.15
2	0.76	0.64	0.25
3	0.76	0.51	0.47
4	0.76	0.41	0.82
5	0.76	0.25	2.17
6	0.51	0.18	8.72
7	0.76	0.25	2.17
8	0.51	0.18	27.58
9	0.89	0.25	55.16

The air compressor is a rotary vane pump using four carbon vanes. The rotor is attached to the shaft of a PMI Model U9M4T printed motor, shown in Figure 20. Supply pressure from the compressor is regulated by controlling the compressor-motor speed with an electronic control using pressure feedback. The block diagram and the schematic are shown in Figures 21 and 22, respectively. The control circuit uses power supplied by the tank's batteries. The added load on the electric system is approximately five amps per axis.

The 24 Vdc nominal supply is regulated to 12 Vdc with a solid-state voltage regulator. The 12 Vdc supply is then used as a reference. The output of a National Semiconductor Model LX1602 solid-state pressure transducer is compared to the reference, amplified, and dynamically compensated. This signal is then used to pulse duration modulate a rectangular wave generator producing a rectangular wave whose on-time is inversely proportional to pressure (pulse duration modulated). The rectangular wave is then power amplified to drive the motor, maintaining the compressor output pressure constant.

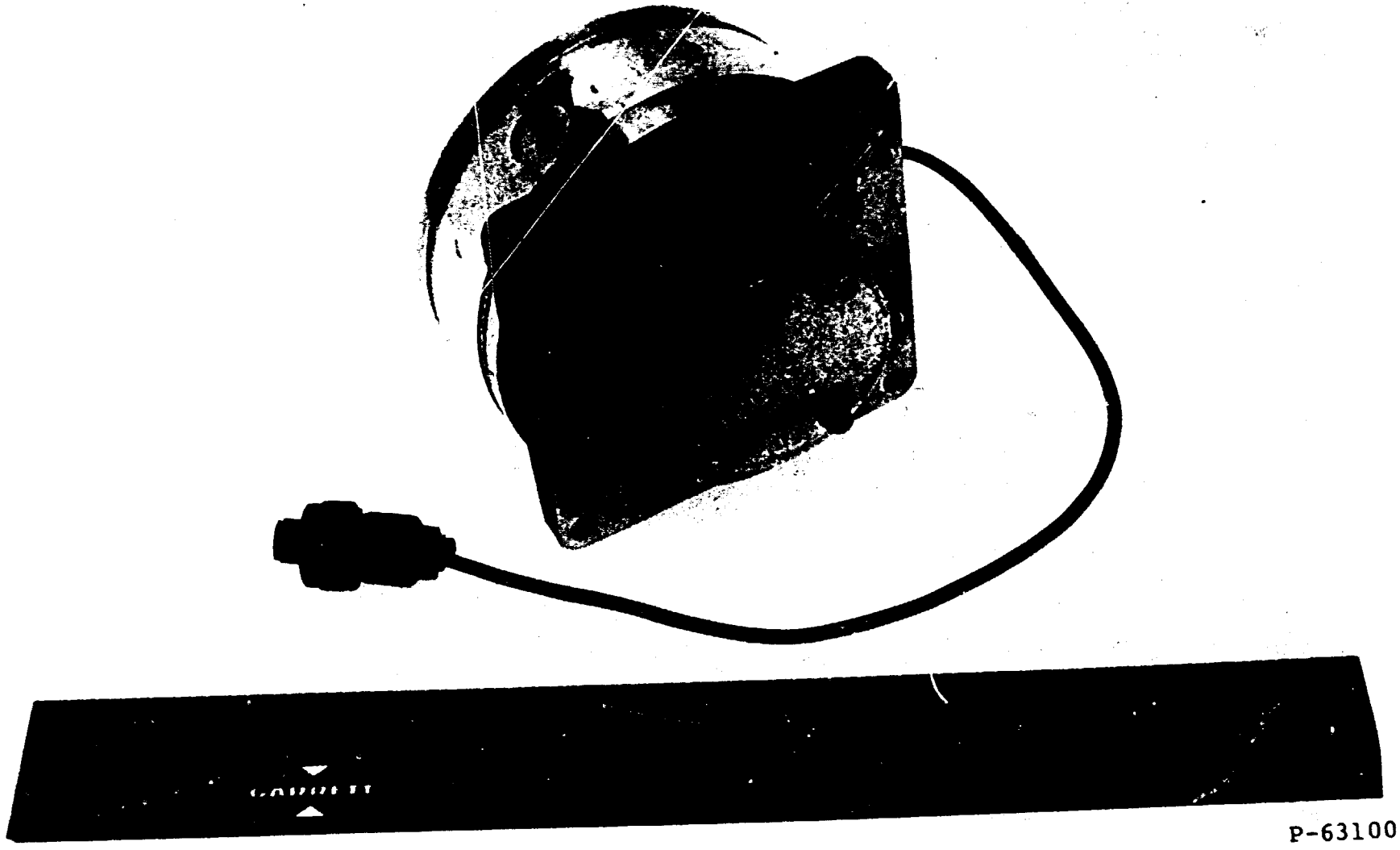

P-63100-9

Figure 20. Motor-compressor assembly.

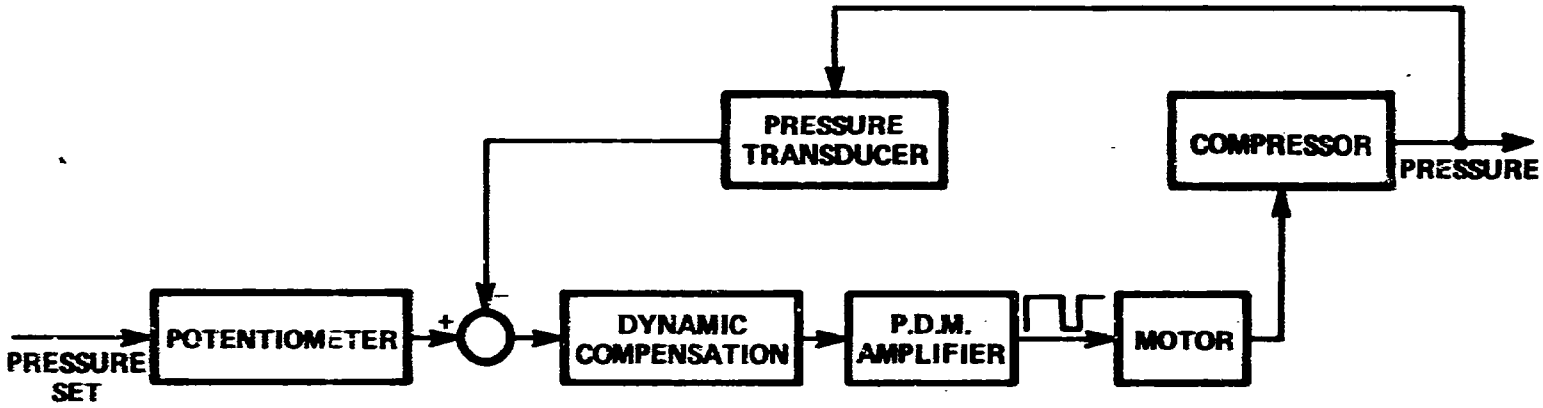

Figure 21. Compressor speed control block diagram.

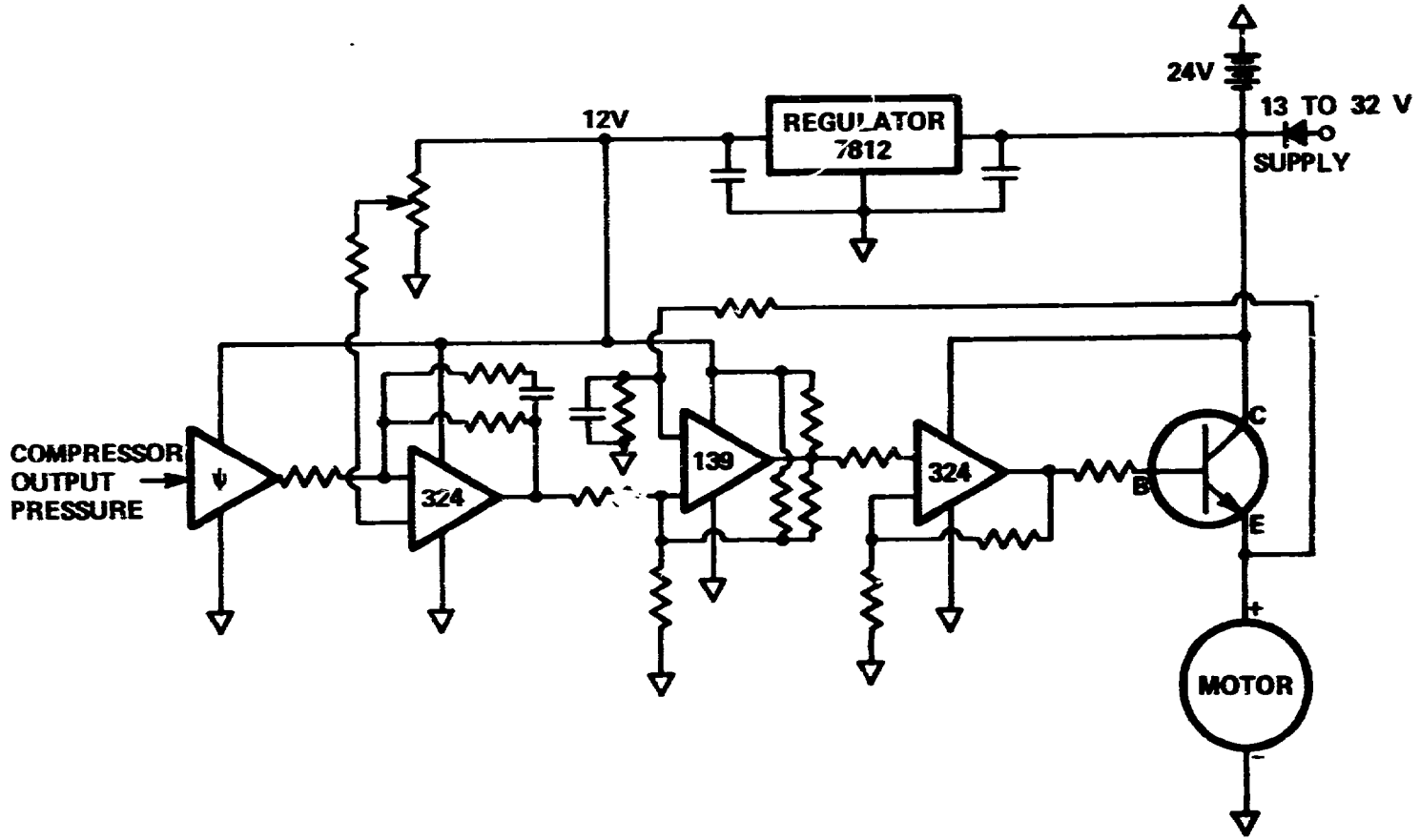

Figure 22. Compressor speed control schematic diagram.

3.4 Fluidic Input Servovalves

Standard electrohydraulic servovalves were adapted to accept pneumatic input signals. For the azimuth axis, a Moog Model 35 flow control valve was used, with a Moog Model 15 pressure control valve used on elevation. The coils and magnets were removed from both valve bodies, leaving the feedback flapper valves installed. A diaphragm assembly was installed in place of the electrical parts. The fluidic output pressure applies force to the diaphragms which, in turn, drive the armature (flapper valve). This concept is shown in Figure 23.

A requirement of the diaphragm drive was sufficient gain (hydraulic valve saturation at fluidic output, ΔP_o = 7 kPa) with negligible phase shift. This requirement was met with a diaphragm area of 3.22 cm^2 (0.5 $in.^2$). Diaphragm displacement necessary to drive the valve full open is approximately 0.076 mm (0.003 in.).

The hysteresis inherent in the hydraulic spool valves, although within the manufacturer's specifications, was excessive for this application. A dither signal applied to the servovalves eliminated the excessive hysteresis. The dither signal was generated with a fluidic oscillator circuit (refer to Figures 3 and 4), operating at approximately 30 Hz. The dither signal is separated from the rate signal with a diaphragm. The diaphragm transmits pulses from the oscillator to the rate signal, but prevents any net flow between oscillator and the rate signal that might affect the rate signal. The dither amplitude is adjusted by varying the supply pressure to the oscillator and is set at a value slightly less than that necessary to obtain gun or turret motion resulting from the 30 Hz signal.

3.5 Handle Position Sensor

During operation in the unstabilized mode, the gunner's handle mechanically positions hydraulic spool valves where one valve supplies hydraulic power to the elevation actuator and the other supplies power to the azimuth hydraulic motor. To enable the gunner to track a moving target during operation in a stabilized mode, hardware was designed that mechanically sensed the gunner's power handle displacement from center (null) position.

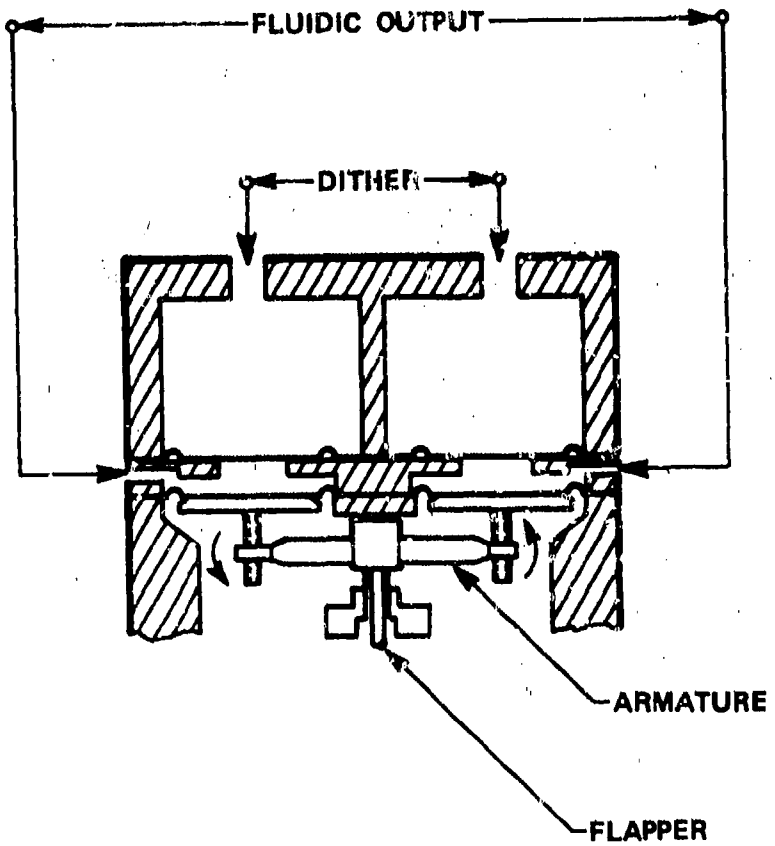

Figure 23. Pneumatic input portion of fluidic-hydraulic servovalves.

Two linkage arms clamp directly to the spools of the power valves. As either spool is moved from its null (off) position, the linkage arms move a cylindrical cam along its axis. Figure 24 shows the cutaway cam and linkage. A cam follower then transmits the cam motion, through a mechanical linkage, to a reverse flow flapper nozzle which, in turn, produces a differential pressure output that is a function of valve position. The pneumatic ΔP from the flapper nozzle is then summed with the rate signal in the fluidic stack.

The cam profile and linkage assembly were designed so that the ΔP_o with respect to spool position had the same nonlinearities as the rate versus spool position resulting from hydraulic shaping. Rate versus spool position shaping was determined from Reference 1. The shaped handle position signal (gunner's commanded rate) is compared to the rate sensor output. As a result, only those rates not commanded by the gunner will be attenuated by the controller.

Precise shaping of the cams was found to be critical near the center (null) position for accurate tracking.

3.6 Notch Filter

The response of the elevation actuation system to a test signal displayed a severe structural resonance at 19 Hz (see Figure 10) due to gun bending. An effort was started to build a notch filter to attenuate the signal at the resonant frequency, thereby preventing the possibility of system instability at 19 Hz. An all-fluidic notch filter was investigated by HDL and a laboratory breadboard circuit was built up that approximated the required notch function. However, when the stabilization system components were ready for installation in the vehicle, the notch filter was not ready for incorporation, so the system was installed and testing was started. As testing progressed and dynamic compensation was being performed, no system instability was observed at the gun resonant frequency. Since the work on the notch filter was done to eliminate an instability at 19 Hz, that effort was stopped shortly after testing on the vehicle began.

---

[1] Kaminski, A. P., "A Mathematical Representation of the M60A1 Azimuth and Elevation Control and Add-On Stabilization System." System Analysis, Defense Division, Chrysler Corporation, Technical Report No. CDE-SA-TR-71-09, 2 November 1971.

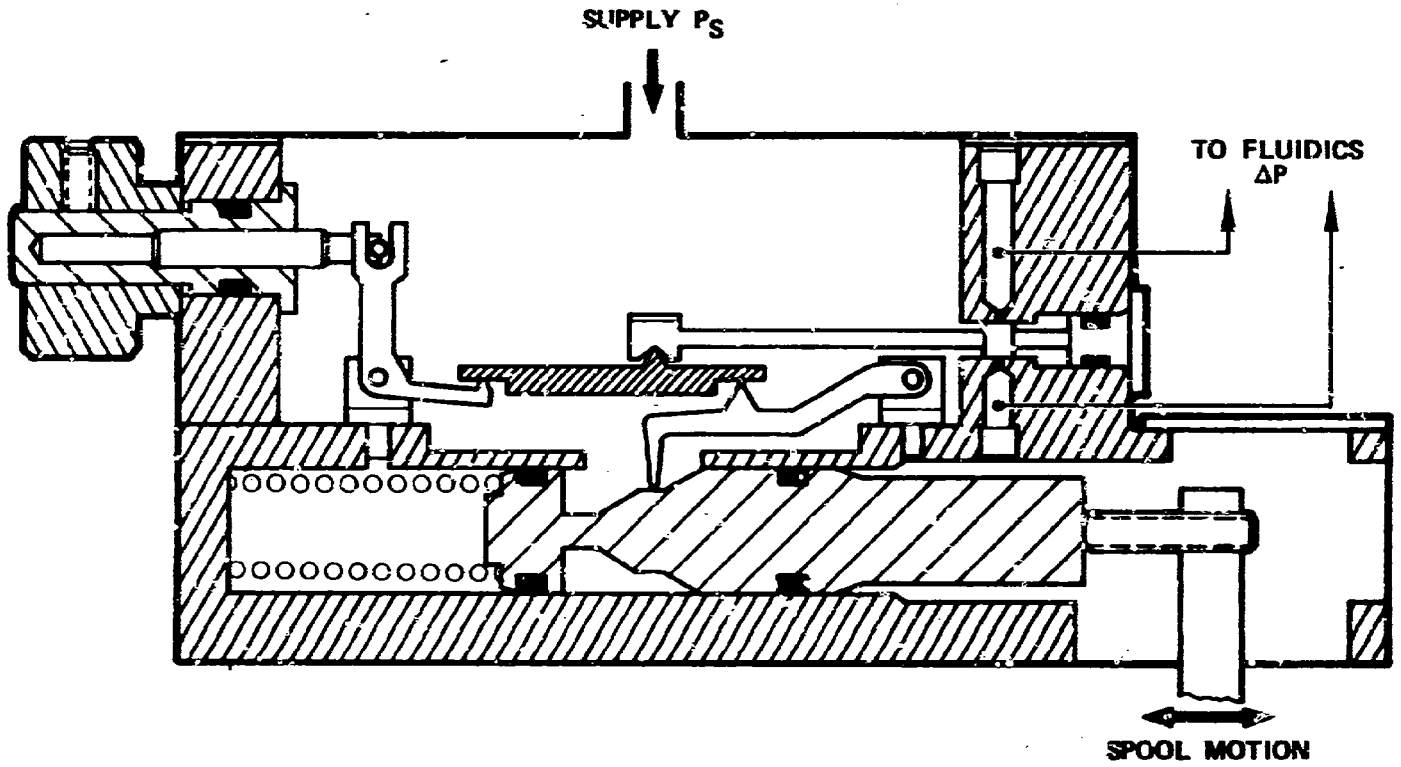

Figure 24. Gunner's handle position sensor.

The reason for absence of the predicted instability is not clearly understood; however, it is probably due to many factors, among which are:

1. Approximately 6 dB of mechanical resonance in the gyro used to measure the gun motion.

2. Rapid nonlinear roll-off characteristics of the fluidic resistors used for dynamic compensation.

3. A small amount of decoupling between the gun and the control unit through the hydraulic actuator where the control was mounted.

4. ON-VEHICLE TESTING

Testing was performed with the fluidic stabilization system installed in an M48A5 tank (see Figure 25) at the Garrett-AiResearch laboratory test facility at Phoenix, Arizona. Frequency response tests were performed by installing a Moog Model 31 electrohydraulic flow control servovalve in parallel with the stabilization servovalve for each axis. By exciting the electrohydraulic servovalve with the oscillating output of a frequency response analyzer, hull motions could be simulated. The resulting motion of the gun and the turret was measured with the rate gyroscopes of the existing hydraulic stabilization system. The test setup schematic is illustrated in Figure 26. The disturbance suppression ratios for the azimuth and elevation axes are plotted versus disturbance frequency as shown in Figures 27 and 28. Also shown for comparison is the performance data for the electrohydraulic add-on stabilization system now used on the M60 battle tank.

Measurements were made on the system also while the tank was undergoing single-axis maneuvers. Results of five repetitions of the aim retention test specified in Reference 2 are tabulated in Table II. All data were within the specified limits. A short bump course, shown in Figure 25, was constructed and utilized to conduct qualitative testing and to provide visual demonstrations to military personnel.

---

[2] "Vehicle Specification, Tank, Combat, M60A1 11655316 Rev. C," Paragraph 4.4.32.1.11, U.S. Army Tank Automotive Command.

Figure 25. M48A5 tank.

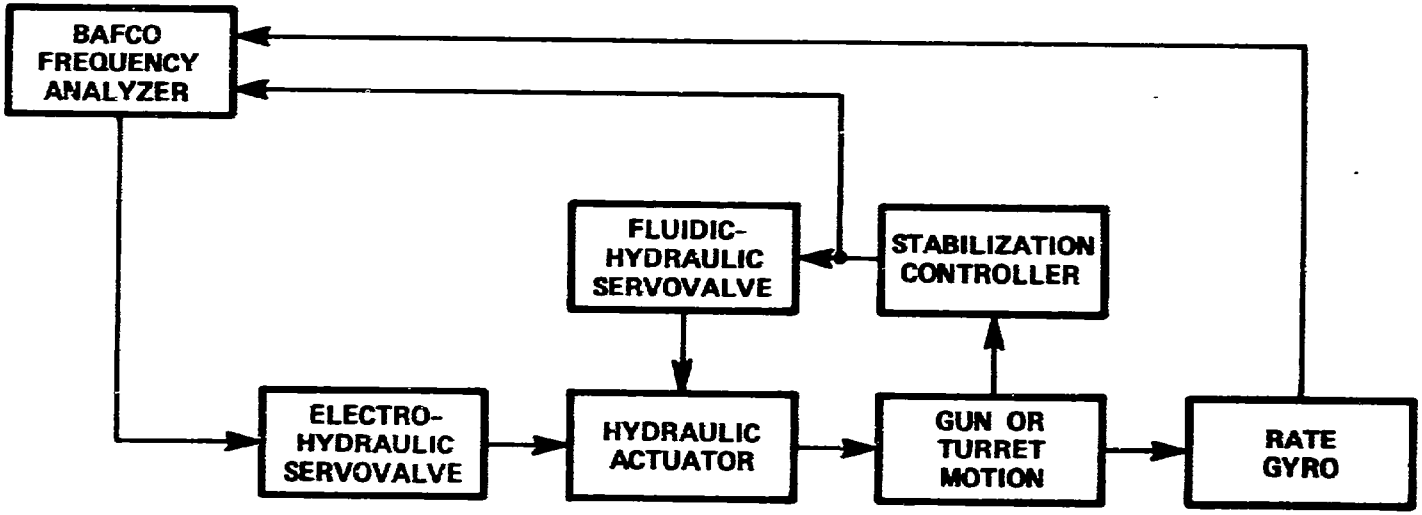

Figure 26. Frequency response test setup.

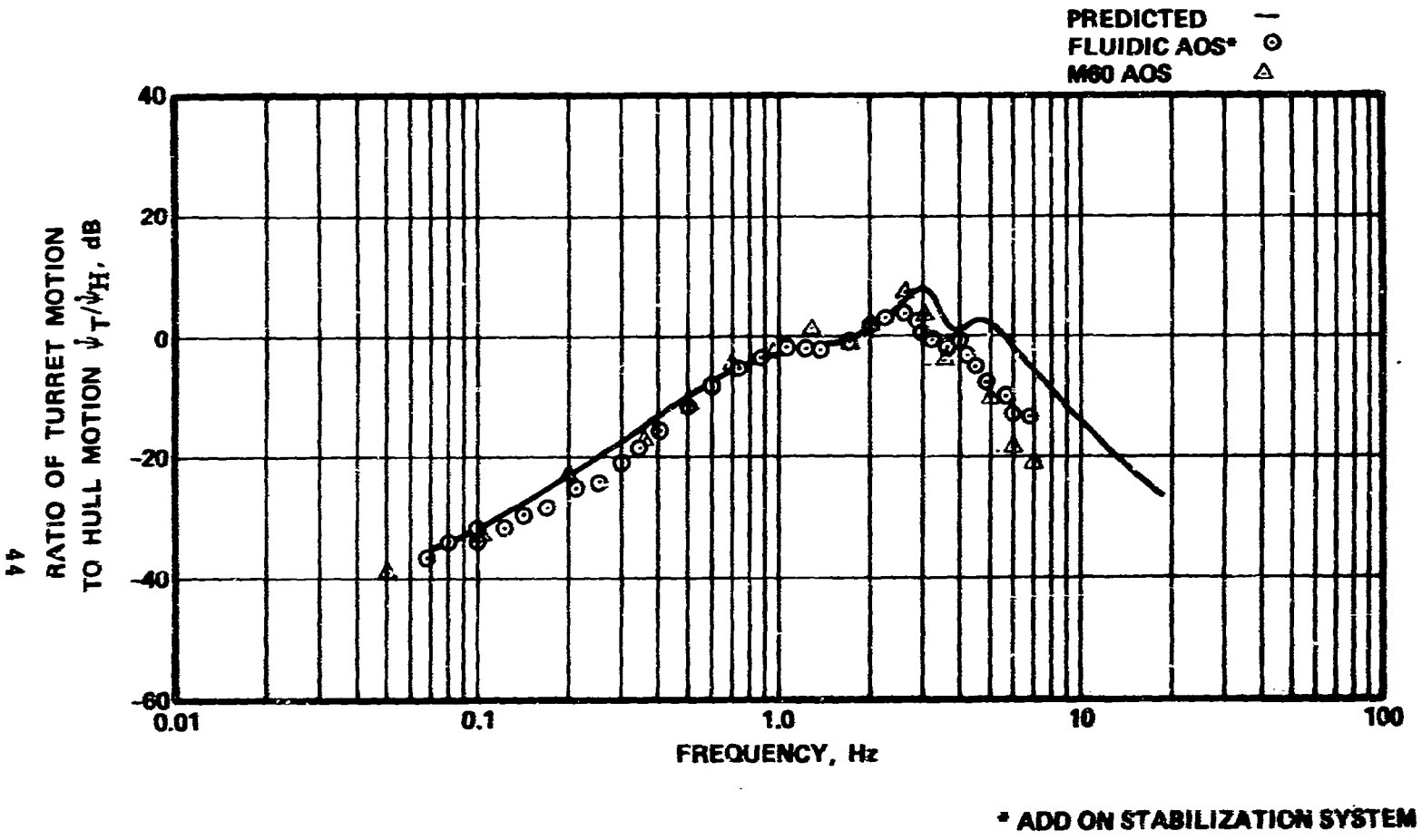

Figure 27. Predicted and actual closed loop responses of azimuth system.

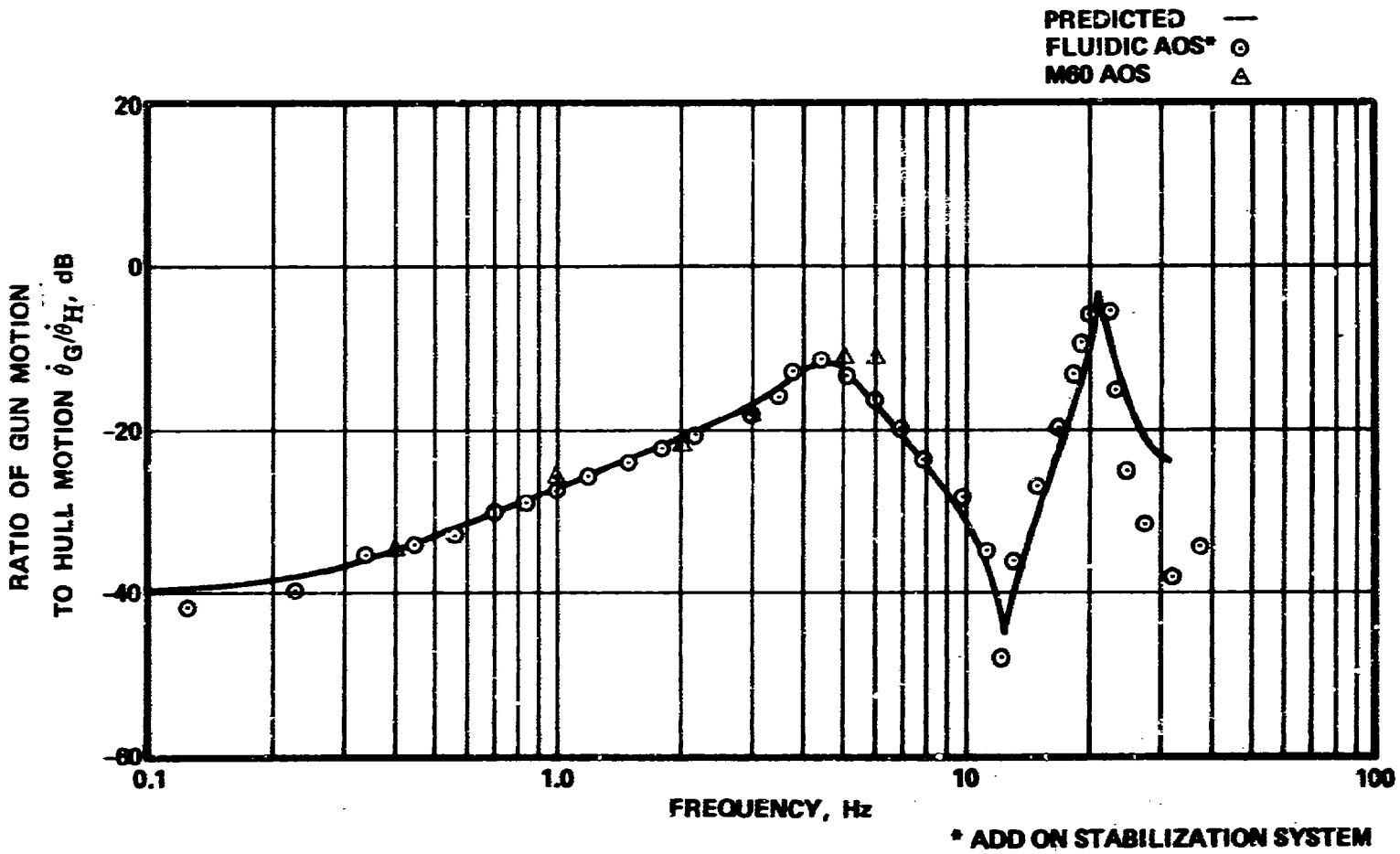

Figure 28. Predicted and actual closed loop responses of elevation system.

TABLE II. ROLL DOWN AND PIVOT TURN DATA

Run No.	Elevation Pull off (mils) (6 mils maximum)	Final (mils) (3 mils maximum)
1	5	2
2	6	2
3	4	1
4	5	2
5	4	1

Run No.	Azimuth Pull off (mils) (9 mils maximum)	Final (mils) (3 mils maximum)
1	9	4
2	8	3
3	8	4
4	9	4
5	7	3

Test performed per Reference 2, Paragraph 4.4.32.1.11

Null drift and a reduction of system gain were encountered as excessively high temperatures were reached during extended periods of operation. Temperature compensation of the fluidic circuits was not attempted during this program phase.

5. RELIABILITY STUDY

A reliability analysis based upon field data conservatively extrapolated to gun stabilization requirements was conducted.[3]

Projected reliability of the fluidic gun stabilization system is shown in Table III.

TABLE III. PROJECTED RELIABILITY

Component or subassembly	Estimated failures per 10 hours	Reliability MTBF hours
Elevation or azimuth		
Fluidic circuit	2	500,000
Servovalve	20	50,000
Standby valve	10	100,000
Vane compressor assembly	50	20,000
Pilot check valves (2 required)	10	100,000
Null adjust	5	200,000
Total for each axis	97	10,309
Double for both	194	5,155
Gunners handle control assembly	20	50,000
Antibacklash cylinder	10	100,000
Hydraulic shutoff valve	20	50,000
Filter for hydraulic system	10	100,000
	254	3,937 hr MTBF

[3] W. T. Fleming and H. R. Gamble, "Reliability Data for Fluidic Systems," AiResearch Manufacturing Co. of Arizona, Phoenix, AZ, HDL-76-092-1 (December 1976).

6. CONCLUSIONS AND RECOMMENDATIONS

The concept of fluidic angular rate sensing and control of turret and gun actuation systems to provide stabilization has been shown to have the capability to meet aim retention specifications written for the electrohydraulic add-on stabilization systems currently in use on the M60A1 tank. The technology base now exists to permit user commands to undertake development programs for specific vehicles without undue technological risk.

Several areas should be focal points of subsequent development efforts.

- Circuit compensation for gain and offset could extend specified performance over more severe environmental conditions.

- A more accurate match of the shaping of the gunner's handle position signal to the gunner's hydraulic valve profile could improve target tracking performance.

- The pneumatic compressor used during this program to supply the fluidic circuits was an adaptation of a readily available commercial design and was deficient in several respects. An improved power supply design could reduce the output noise and also reduce the wear products, both of which were encountered to some degree. A broadly oriented program to develop a compact, efficient, and reliable pneumatic power supply tailored to the requirements of fluidic circuits in general should be undertaken.

- Due to present controller designs, separate testing of the pneumatic and hydraulic components is not convenient. Modular construction would allow the fluidic controllers to be removable without disturbing hydraulic connections and thereby permit easy removal for adjustment and calibration.

- Advanced vehicles currently under development require communication between the gun stabilization system and other vehicle

systems such as stabilized sights and electronic fire control computers. A program for evaluation of existing and proposed pneumatic to electronic interface devices should be initiated so that the advantages of fluidic rate sensing and control could be extended to these other vehicle systems.

- Cost analyses have shown that nonfluidic system components govern system cost. Hydraulic servovalves are traditionally expensive components that could perhaps benefit from incorporation of fluidic technology. It is recommended that servovalve programs be established.

SYMBOLS

b_s = power jet nozzle width

G_E = elevation actuation system transfer function

G_T = azimuth actuation system transfer function

H_E = elevation controller transfer function

H_T = azimuth controller transfer function

h = power jet nozzle height

J_G = gun moment of inertia

J_H = hull moment of inertia

J_T = turret moment of inertia

$K = 3.33 \times 10^{-4}$ s

K_L = system loop gain

N_R = Reynolds number

P_s = supply pressure

ΔP = differential pressure

ΔP_o = differential output pressure

P_1 = inlet pressure

S = Laplace transform variable

X_{sp} = power nozzle exit to splitter distance

α = jet bending angle

ζ_G = gun barrel damping ratio

ζ_H = hull suspension damping ratio

ζ_T = turret drive damping ratio

$\dot{\theta}$ = angular velocity

$\dot{\theta}_C$ = commanded angular velocity of gun

$\dot{\theta}_G$ = angular rate of gun in elevation axis

PRECEDING PAGE BLANK-NOT FILMED

$\dot{\theta}_H$ = angular velocity of hull in elevation axis

$\dot{\theta}_V$ = angular rate command to servovalve

ν = kinematic viscosity

$\dot{\psi}_C$ = commanded angular velocity of turret

$\dot{\psi}_H$ = angular velocity of hull in azimuth axis

$\dot{\psi}_T$ = angular velocity of turret

$\dot{\psi}_V$ = angular velocity command to servovalve

ρ = fluid density

τ_1, τ_2 = azimuth axis dynamic compensation lead time constants

τ_3, τ_4 = azimuth axis dynamic compensation lag time constant

τ_5 = response time constant of servovalve input diaphragms, and associated pneumatic ducting

τ_6, τ_7 = elevation axis dynamic compensation lead time constants

τ_8, τ_9 = elevation axis dynamic compensation lag time constants

τ_e = empirical transport delay

τ_G = servovalve droop time constant

τ_r = transport delay time associated with rate sensor and fluidic amplifier

ω_G = gun barrel resonant frequency

ω_H = hull suspension natural frequency in the azimuth axis

ω_T = turret drive natural frequency

DISTRIBUTION

Defense Documentation Center
Cameron Station, Building 5
Alexandria, VA 22314
ATTN: DDC-TCA (2 copies)

Director
Applied Technology Laboratory
Fort Eustis, VA 23604
ATTN: George W. Fosdick, DAVDL-EU-SYA

Commander
USA Missile Res & Dev Command
Redstone Arsenal, AL 35809
ATTN: DRDMI-TGC, William Griffith
ATTN: DRDMI-TGC, J. C. Dunaway

Commander
USA Mobility Equipment R&D Center
Fort Belvoir, VA 22060
ATTN: DRDME-EM, R. N. Ware

Commander
US Army ARRADCOM
Dover, NJ 07801
ATTN: DRDAR-LCN-F, A. E. Schmidlin
ATTN: DRDAR-LCW-E, Mr. J. Connors
ATTN: DRDAR-LCW, Mr. R. Wrenn
ATTN: DRDAR-SCF, Mr. J. Schmitts

Commander
USA Tank Automotive Res & Dev Command
Armor & Comp Div, DRDTA-RKT
Building 215
Warren, MI 48090
ATTN: T. Kozowyk
ATTN: M. Steele
ATTN: DRDTA-RCA
ATTN: DRDTA-RC, Mr. E. R. Jackovich
ATTN: DRDTA-RCAF, Mr. A. Farkas
ATTN: DRDTA-ZE, Mr. C. Bradley
ATTN: Col. H. H. Dobbs, Dir., TASL

DISTRIBUTION (CONT'D)

Commander
Naval Air Development Center
Warminster, PA 18974
ATTN: R. McGiboney, 30424

Naval Air Systems Command
Department of the Navy
Washington, DC 0360
ATTN: CODE AIR-52022J, D. Houck

Director
US Army Materiel Systems Analysis Agency
Aberdeen Proving Ground, MD 21005
ATTN: DRXSY-GA, Mr. G. Zeller

HQ, DARCOM
German Liaison Office
5001 Eisenhower Ave.
Alexandria, VA 22333
ATTN: Mr. Sellmer

Commander
US Army ARRADCOM
Watervliet, NY 12189
ATTN: DRDAR-LCD, Mr. F. John

Office of the Deputy Chief of Staff for Res, Dev, & Acquisition
Department of the Army
Washington, DC 20310
ATTN: DAMA-CSZ, Dr. Henry Smith

Commander ODDR&E
Pentagon, Room 3D1089
Washington, DC 20310
ATTN: George C. Kopcsak

Director of Combat Development
HQ, US Army Armor Center
Ft. Knox, KY 40121
ATTN: ATZK-CD-SD
ATTN: ATZK-CD-MS

DISTRIBUTION (CONT'D)

Commander
US Army Armor Center
Ft. Knox, KY 40121

Project Manager, M60 Tank Development
DRCPM-M60TD
Warren, MI 48090

Commander
Naval Ship Engineering Center
Philadelphia Division
Philadelphia, PA 19112
ATTN: CODE 6772, D. Keyser

Commander
Air Force Flight Dynamics Laboratory
Wright-Patterson AFB, OH 45433
ATTN: AFFDL/FGL, H. Snowball

Harry Diamond Laboratories
ATTN: Chief, Div 10000
ATTN: Chief, Lab 13000
ATTN: Public Affairs Office
ATTN: Record Copy, 94100
ATTN: HDL Library, 41000 (3 copies)
ATTN: Chairman, Editorial Committee
ATTN: Technical Reports Branch, 41300
ATTN: Chief, 13400 (35 copies)

APPENDIX A.--RATE SENSOR AND AMPLIFIER DIMENSIONAL DESCRIPTION

Figure A-1 defines the profile of the laminate proportional amplifiers used for amplification of the angular rate signal.

Figure A-2 delineates the profile of the angular rate sensor used in the stabilization system.

Figures A-3, A-4, and A-5 are computer-generated drawings identifying the features of the rate sensor profile; "L" designations are lines and "A" designations are arcs.

Table A-I is a list of the coordinate data associated with the features designated in Figures A-3, A-4, and A-5. Coordinate reference point is the center of A-1; that is X = 0, Y = 0.

All dimensions given in Appendix A are in inches.

PRECEDING PAGE BLANK-NOT FILMED

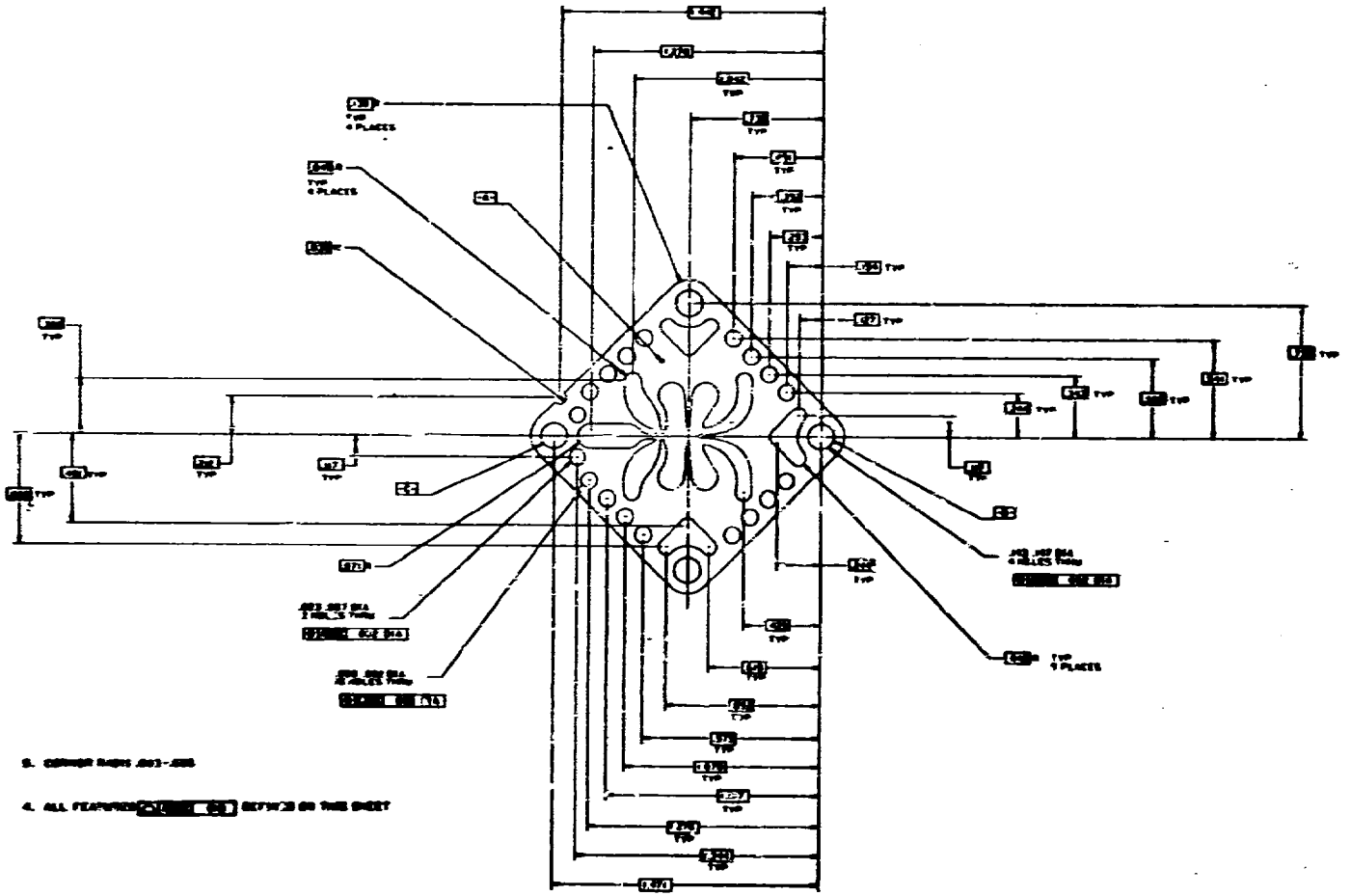

Figure A-1. Fluidic amplifier element.

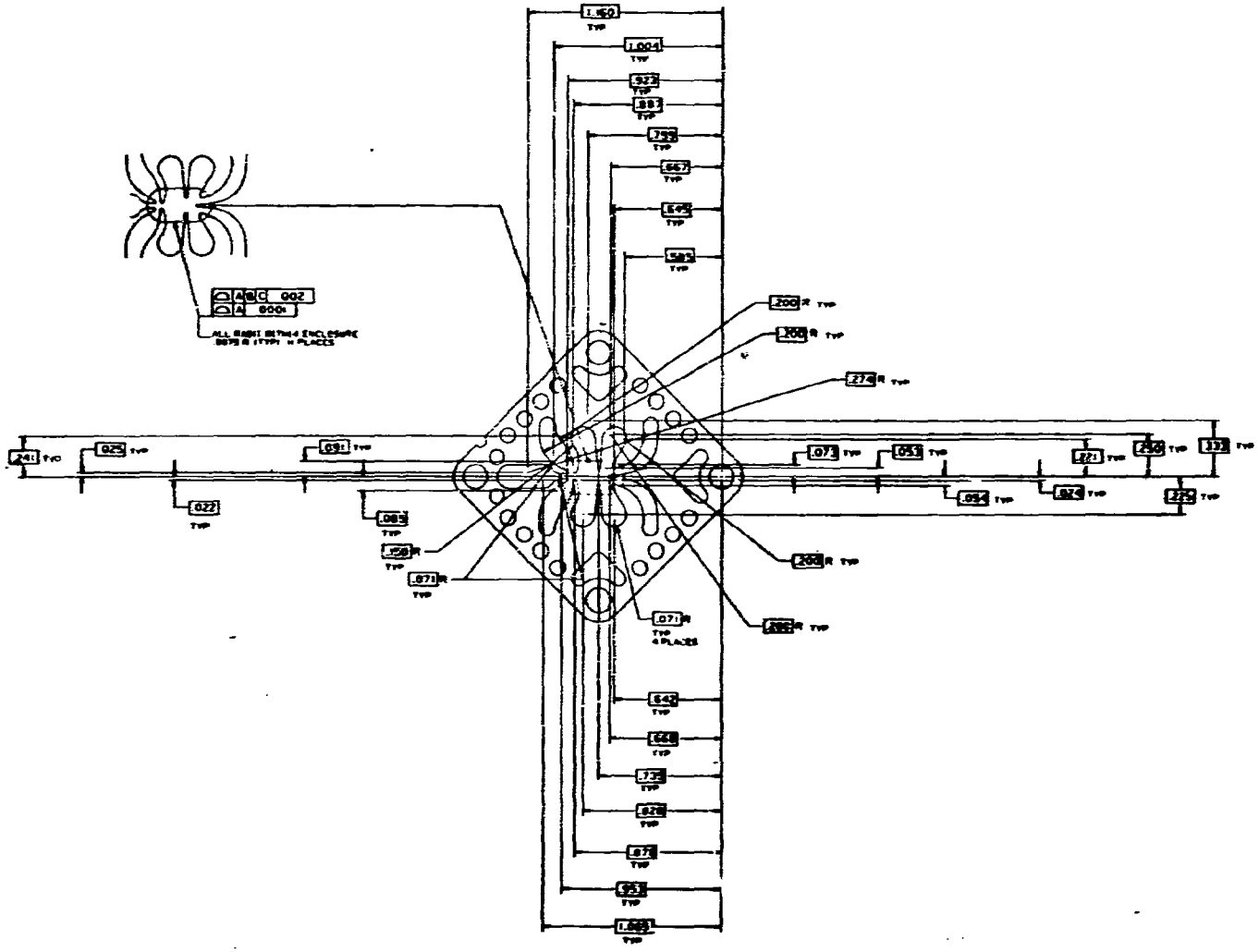

Figure A-1. Fluidic amplifier element (cont).

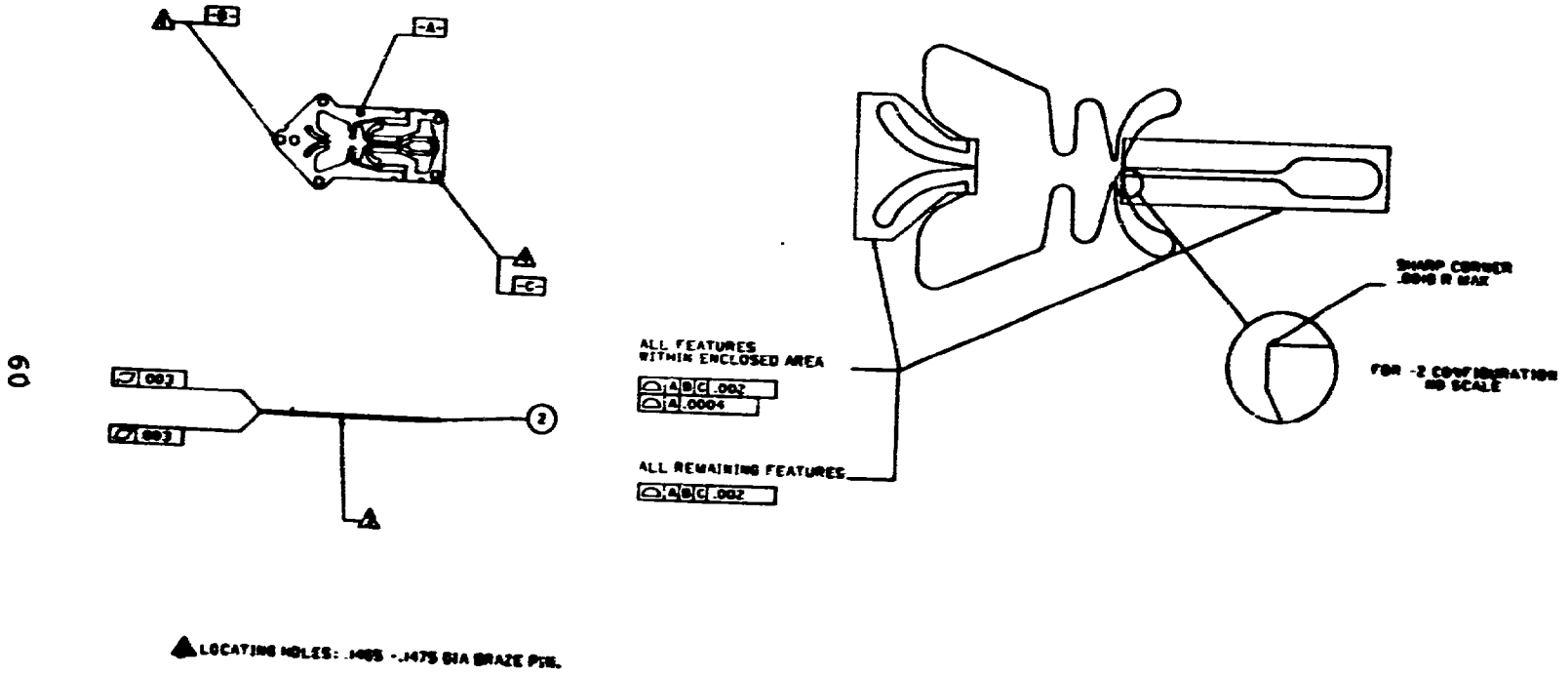

Figure A-2. Rate sensor element.

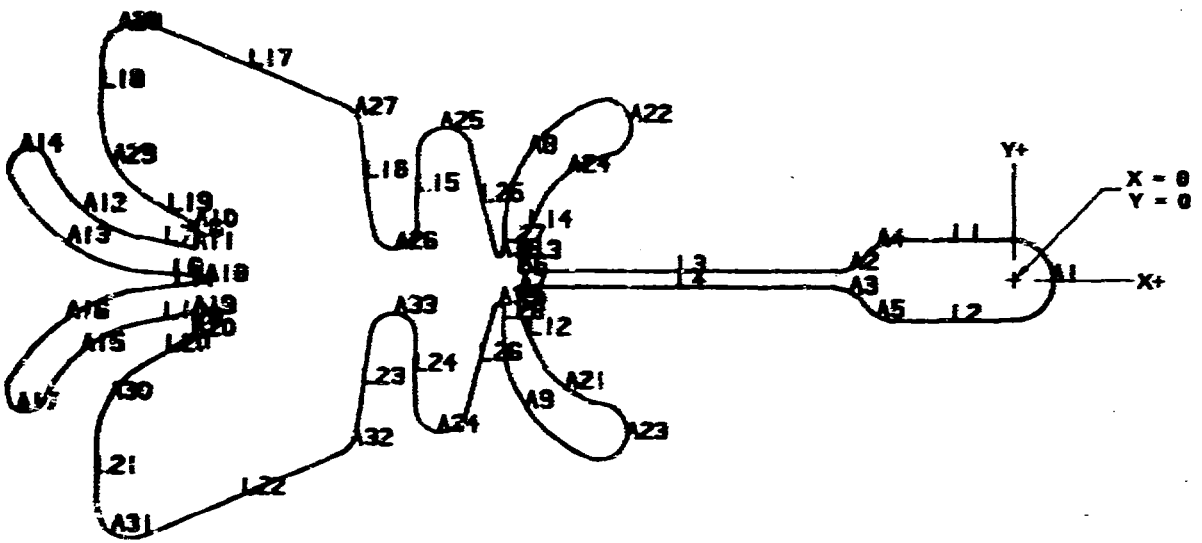

Figure A-3. Rate sensor profile identification.

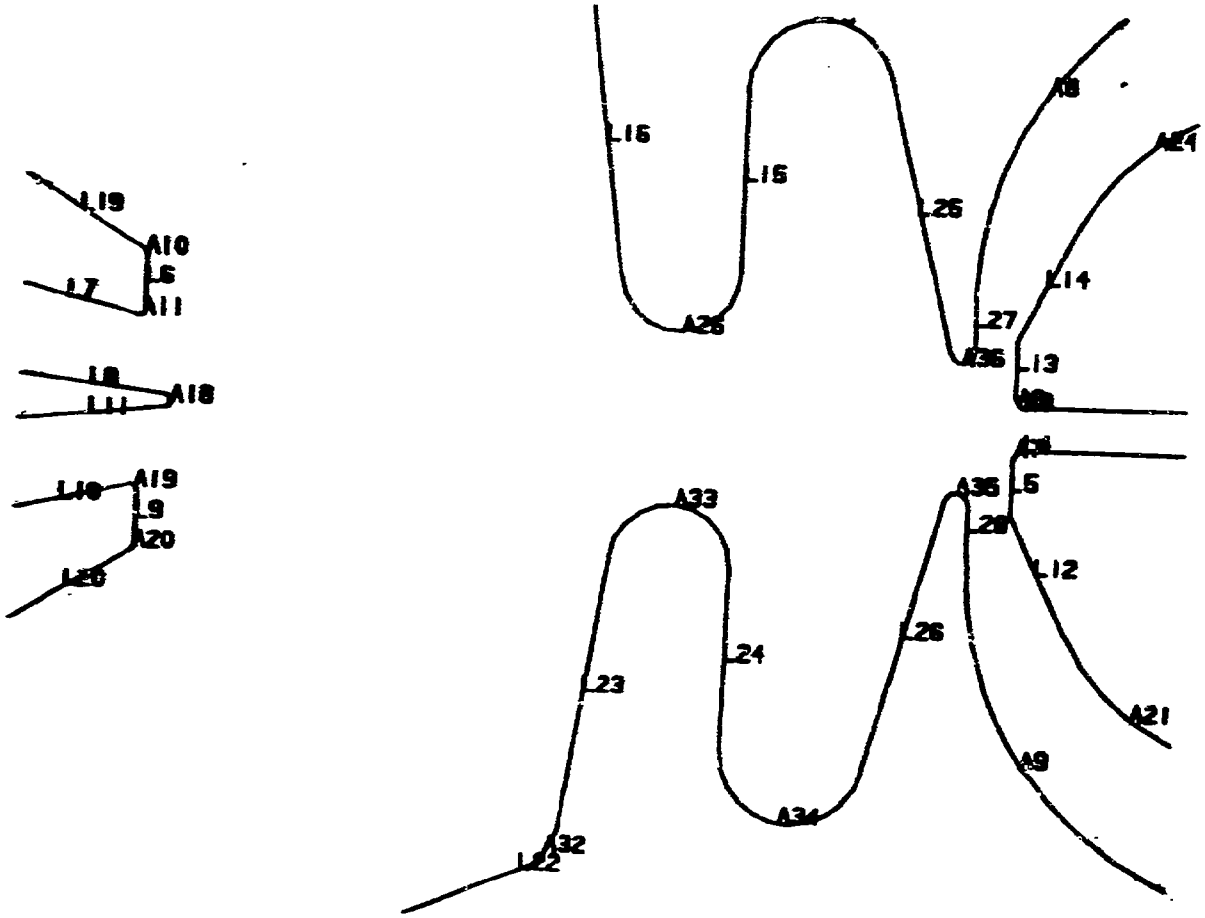

Figure A-4. Rate sensor profile identification.

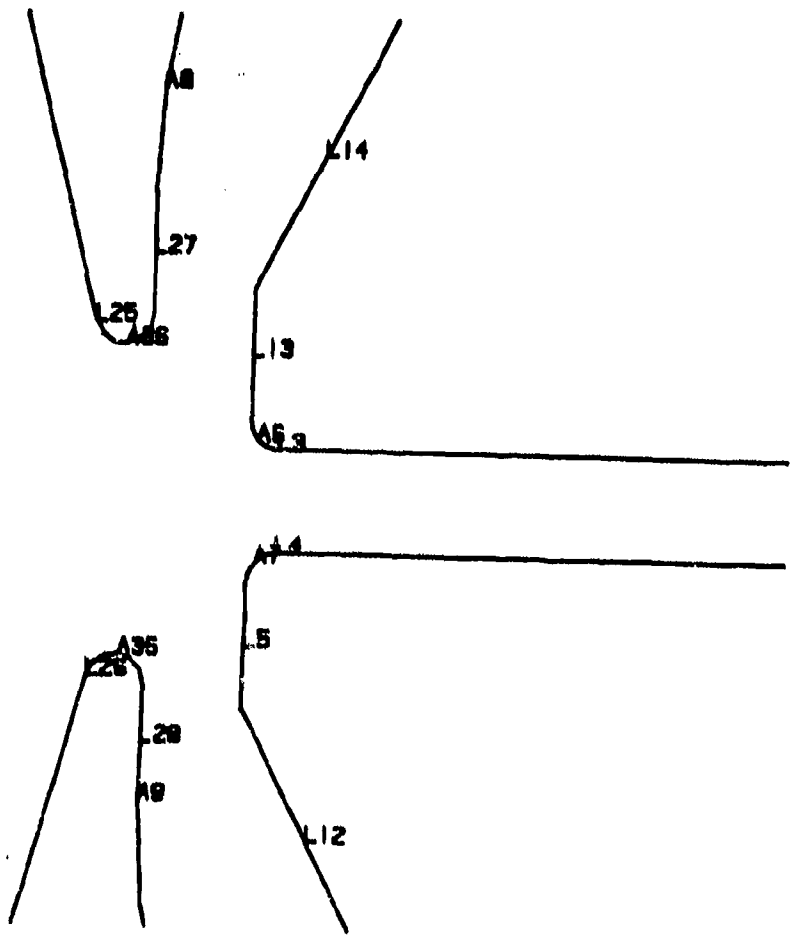

Figure A-5. Rate sensor profile identification.

TABLE A-I. COORDINATED DATA.

Name	End point 1	End point 2
L1	X1 = -0.25900001 Y1 = 0.08750000	X2 = 0.0000 Y2 = 0.08750000
L2	X1 = -0.2590001 Y1 = -0.08750000	X2 = 0.0000 Y2 = -0.08750000
L3	X1 = -0.3951983 Y1 = 0.01750000	X2 = -1.085000 Y2 = 0.01750000
L4	X1 = -0.3951983 Y1 = -0.01750000	X2 = -1.085000 Y2 = -0.01750000
L5	X1 = -1.095000 Y1 = -0.02750000	X2 = -1.095000 Y2 = -0.07100000
L6	X1 = -1.820000 Y1 = 0.07400000	X2 = -1.820000 Y2 = 0.1170000
L7	X1 = -1.826040 Y1 = 0.06910927	X2 = -1.944686 Y2 = 0.09432953
L8	X1 = -1.799478 Y1 = 0.004972618	X2 = -1.927503 Y2 = 0.01842627
L9	X1 = -1.820000 Y1 = -0.1170000	X2 = -1.820000 Y2 = -0.07400000
L10	X1 = -1.826040 Y1 = -0.06910926	X2 = -1.944684 Y2 = -0.09432860
L11	X1 = -1.799478 Y1 = -0.004972612	X2 = -1.927509 Y2 = -0.01842830
L12	X1 = -1.095000 Y1 = -0.07100000	X2 = -1.047540 Y2 = -0.1640590
L13	X1 = -1.095000 Y1 = 0.02750000	X2 = -1.095000 Y2 = 0.07100000
L14	X1 = -1.095000 Y1 = 0.07100000	X2 = -1.047540 Y2 = 0.1640590

TABLE A-I. COORDINATED DATA (CONT'D).

Name	End point 1	End point 2
L15	X1 = -1.325000 Y1 = 0.2700000	X2 = -1.325000 Y2 = 0.1200000
L16	X1 = -1.424529 Y1 = 0.1131491	X2 = -1.455471 Y2 = 0.3368510
L17	X1 = -1.922255 Y1 = 0.5578561	X2 = -1.485784 Y2 = 0.3761601
L18	X1 = -2.033000 Y1 = 0.4840000	X2 = -2.033000 Y2 = 0.3583321
L19	X1 = -1.822500 Y1 = 0.1213301	X2 = -1.933000 Y2 = 0.1851269
L20	X1 = -1.822500 Y1 = -0.1213301	X2 = -1.933001 Y2 = -0.1851278
L21	X1 = -2.033000 Y1 = -0.4840000	X2 = -2.033000 Y2 = -0.3583327
L22	X1 = -1.922255 Y1 = -0.5578561	X2 = -1.485784 Y2 = -0.3761601
L23	X1 = -1.455471 Y1 = -0.3368510	X2 = -1.424529 Y2 = -0.1131491
L24	X1 = -1.325000 Y1 = -0.2700000	X2 = -1.325000 Y2 = -0.1200000
L25	X1 = -1.149692 Y1 = 0.06003524	X2 = -1.206851 Y2 = 0.2847885
L26	X1 = -1.149692 Y1 = -0.06003524	X2 = -1.206851 Y2 = -0.2847885
L27	X1 = -1.130000 Y1 = 0.06250000	X2 = -1.130000 Y2 = 0.1037259
L28	X1 = -1.130000 Y1 = -0.1037257	X2 = -1.130000 Y2 = -0.06250000

TABLE A-I. COORDINATED DATA (CONT'D).

Name	Radius	Center	Start angle	End angle
A1	0.08750000	X = 0.0000 Y = 0.0000	270.0000	450.0000
A2	0.08000000	X = -0.3951983 Y = 0.9750000	270.0000	324.4024
A3	0.08000000	X = -0.3951983 Y = -0.09750000	35.59763	90.00001
A4	0.8750000	X = -0.2590001 Y = 0.0000	90.00001	144.4024
A5	0.08750000	X = -0.2590001 Y = 0.0000	215.5976	270.000
A6	0.01000000	X = -1.085000 Y = 0.2750000	180.0000	270.0000
A7	0.01000000	X = -1.085000 Y = -0.2750000	90.00001	180.0000
A8	0.3000000	X = -0.8299999 Y = 0.1037258	109.4712	180.0000
A9	0.03000000	X = -08299999 Y = -1.1037258	180.0000	250.5288
A10	0.005000000	X = -1.825000 Y = 0.1170000	0.0000	60.00062
A11	0.005000000	X = -1.825000 Y = 0.07400000	257.9992	360.0000
A12	0.3000000	X = -1.882310 Y = 0.3877733	204.9945	257.9995
A13	0.4000000	X = -1.885699 Y = 0.4162358	209.3935	264.0011
A14	0.04499999	X = -2.195000 Y = 0.2420000	24.99446	209.3933

TABLE A-I. COORDINATED DATA (CONT'D).

Name	Radius	Center	Start angle	End angle
A15	0.3000000	X = -1.882309 Y = -0.3877726	102.0003	155.0057
A16	0.4000000	X = -1.885700 Y = -0.4162374	95.99960	150.6062
A17	0.04499999	X = -2.195000 Y = -0.2420000	150.6060	335.0056
A18	0.005000000	X = -1.800000 Y = 0.0000	275.9997	444.0018
A19	0.005000000	X = -1.825000 Y = -0.07400000	0.0000	102.0008
A20	0.005000000	X = -1.825000 Y = -0.1170000	300.0007	360.0000
A21	0.2000000	X = -0.8693728 Y = -0.07319380	207.0216	261.0102
A22	0.06000000	X = -0.9100001 Y = 0.3300000	279.0600	469.4713
A23	0.06000000	X = -0.9100001 Y = -0.3300000	250.5288	441.0102
A24	0.2000000	X = -0.8693728 Y = 0.07319380	98.96876	152.9785
A25	0.06000000	X = -1.265000 Y = 0.2700000	14.26902	180.0000
A26	0.05000000	X = -1.375000 Y = 0.1200000	187.8753	360.0000
A27	0.05000000	X = -1.505000 Y = 0.3300000	7.875351	67.39883
A28	0.08000000	X = -1.953000 Y = 0.4840000	67.39081	180.0000

TABLE A-I. COORDINATED DATA (CONCLUDED).

Name	Radius	Center	Start angle	End angle
A29	0.2000000	X = -1.833000 Y = 0.3583321	180.0000	240.0001
A30	0.2000000	X = -1.833000 Y = -0.3583327	120.0001	180.0000
A31	0.8000000	X = -1.953000 Y = -0.4840000	180.0000	292.6012
A32	0.05000000	X = -1.505000 Y = -0.3300000	292.6012	352.1247
A33	0.05000000	X = -1.375000 Y = -0.1200000	0.0000	172.1247
A34	0.6000000	X = -1.265000 Y = -0.2700000	180.0000	345.7310
A35	0.01000000	X = -1.140000 Y = -0.06250000	0.0000	165.7310
A36	0.01000000	X = -1.140000 Y = 0.6250000	194.2691	360.0000

APPENDIX B.--DETAILED STACKING SEQUENCE

A detailed list of the parts that were used to build the fluidic gain blocks in the azimuth and elevation axis follows. Some part numbers are followed by M, M_1, or M_2, which represent a modification of the standard parts. These modified parts are shown in Figure B-1. All parts have an orientation notch near one corner, as shown on the drawing preceding the parts list. The orientations of the notches are relative to one another and are denoted by a letter in the parts list. The orientation key shows the position assigned to each letter.

The stacking sequence starts from the rate sensor and builds to the final output stage. Each stacking sequence starts with the bottom of the stack and all communication with the stack is made through the bottom.

The gain blocks were divided to form several stacks (two in azimuth and four in elevation) to aid in communicating with the various amplifiers in the cascade. Smaller stacks are made the packaging more flexible.

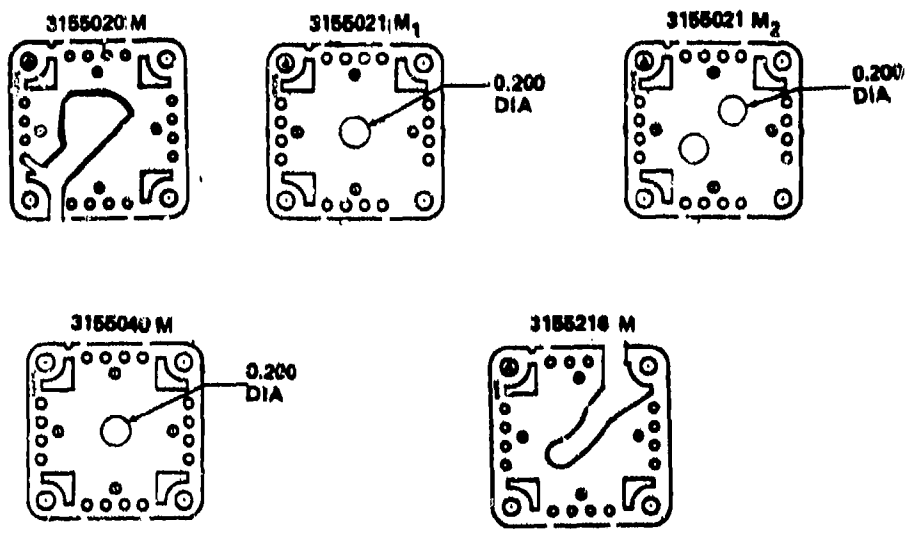

Figure B-1. Modified standard parts.

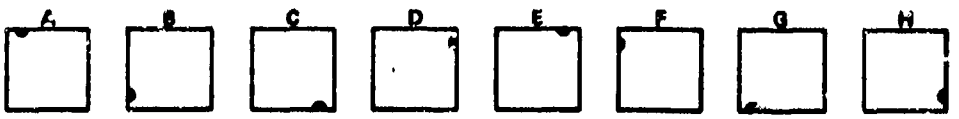

ORIENTATION KEY

AZIMUTH AXIS STACK NO. 1

Stack Sequence	Part Number	Orientation	Description	Quantity Required	Remarks
1	3155033	A	Transfer	5	
2	3155021	H	Gasket	1	
3	3155219	G	Nozzle	1	
4	3155021 M_1	C	Vent	1	Modified part
5	3155219	G	Nozzle	1	
6	3155021 M_1	C	Vent	1	Modified part
7	3155221	B	Nozzle	1	
8	3155021 M_1	C	Vent	1	Modified part
9	3155221	B	Nozzle	1	
10	3155021 M_1	G	Vent	1	Modified part
11	3155221	G	Nozzle	1	
12	3155021 M_1	H	Vent	1	Modified part
13	3155221	B	Nozzle	1	
14	3155021 M_1	H	Vent	1	Modified part
15	3155221	B	Nozzle	1	
16	3155021 M_1	C	Vent	1	Modified part
17	3155221	G	Nozzle	1	
18	3155018	C	Gasket	1	
19	3155018	C	Gasket	1	
20	3155040	F	Gasket	1	
21	3155300	F	Nozzle	6	
22	3155040	F	Gasket	1	
23	3155300	F	Nozzle	6	
24	3155040	F	Gasket	1	
25	3155000	F	Nozzle	6	
26	3155040	F	Gasket	1	
27	3155300	F	Nozzle	6	
28	3155040	F	Gasket	1	
29	3155300	F	Nozzle	6	
30	3155018	H	Gasket	1	
31	3155216	C	Exhaust	2	
32	3155237	C	Exhaust	1	
33	3155236	H	Vent	2	
34	3169138	C	Amp	1	h = 0.032

AZIMUTH AXIS STACK NO. 1 (CONTD)

Stack Sequence	Part Number	Orientation	Description	Quantity Required	Remarks
35	3155236	H	Vent	2	
36	3155237	H	Exhaust	1	
37	3155216	C	Exhaust	2	
38	3155018	A	Gasket	1	
39	3155021	F	Gasket	1	
40	3155300	H	Nozzle	5	
41	3155040	H	Gasket	1	
42	3155300	H	Nozzle	5	
43	3155040	H	Gasket	1	
44	3155300	H	Nozzle	5	
45	3155040	H	Gasket	1	
46	3155300	H	Nozzle	5	
47	3155040	H	Gasket	1	
48	3155300	H	Nozzle	3	
49	3155040	H	Gasket	1	
50	3155191	H	Transfer	2	
51	3155116	C	Transfer	2	
52	3155040	C	Gasket	1	
53	3155020	G	Cap	2	
54	3155040	G	Gasket	1	
55	3155020	D	Cap	2	
56	3155018	A	Gasket	1	
57	3155021	D	Gasket	1	
58	3155044	C	Gasket	1	
59	3155216 M	F	Exhaust	2	Modified part
60	3155237	A	Exhaust	1	
61	3155236	A	Vent	2	
62	3169138	F	Amp	1	h = 0.030
63	3155236	A	Vent	2	
64	3155237	A	Exhaust	1	
65	3155216 M	F	Exhaust		Modified part
66	3155021	H	Gasket	1	
67	3155040	E	Gasket	1	
68	3155221	C	Nozzle	3	
69	3155217	A	Exhaust	1	
70	3155221	H	Nozzle	3	
71	3155040	H	Gasket	1	
72	3155221	H	Nozzle	3	
73	3155217	A	Exhaust	1	
74	3155221	H	Nozzle	3	
75	3155040	H	Gasket	1	

AZIMUTH AXIS STACK NO. 1 (CONTD)

Stack Sequence	Part Number	Orientation	Description	Quantity Required	Remarks
76	3155221	H	Nozzle	3	
77	3155217	A	Exhaust	1	
78	3155219	H	Nozzle	3	
79	3155040	H	Gasket	1	
80	3155219	H	Nozzle	3	
81	3155217	A	Exhaust	1	
82	3155219	H	Nozzle	3	
83	3155018	H	Gasket	1	
84	3155219	H	Nozzle	3	
85	3155217	A	Exhaust	1	
86	3155219	H	Nozzle	3	
87	3155018	H	Gasket	1	
88	3155040	A	Gasket	1	
89	3155021	D	Gasket	1	
90	3155216 M	C	Exhaust	2	Modified part
91	3155237	H	Exhaust	1	
92	3155236	C	Vent	2	
93	3169138	C	Amp	1	h = 0.025
94	3155236	C	Vent	2	
95	3155237	C	Exhaust	1	
96	3155216 M	C	Exhaust	1	Modified part
97	3155018	F	Gasket	1	
98	3155021	A	Gasket	1	
99	3155221	G	Nozzle	1	
100	3155217	H	Exhaust	1	
101	3155219	G	Nozzle	1	
102	3155040	H	Gasket	1	
103	3155219	B	Nozzle	1	
104	3155217	H	Exhaust	1	
105	3155219	G	Nozzle	1	
106	3155040	D	Gasket	1	
107	3155216 M	F	Exhaust	2	Modified part
108	3155237	F	Exhaust	1	
109	3155236	A	Vent	2	
110	3169138	F	Amp	1	h = 0.020
111	3155236	A	Vent	2	
112	3155237	A	Exhaust	1	
113	3155216 M	F	Exhaust	2	Modified part
114	3155018	C	Gasket	1	
115	3155116	G	Transfer	2	
116	3155110	E	Transfer	2	
117	3155019	A	Gasket	5	

AZIMUTH AXIS STACK NO. 2

Stack Sequence	Part Number	Orientation	Description	Quantity Required	Remarks
1	3155034	A	Gasket	1	
2	3155033	A	Transfer	6	
3	3155046	F	Gasket	1	
4	3155038	H	Transfer	2	
5	3155045	F	Gasket	1	
6	3155018	D	Gasket	1	
7	3155035	H	Transfer	3	
8	3155018	G	Gasket	1	
9	3155217	D	Exhaust	4	
10	3155021 M_2	E	Vent	1	Modified part
11	3155237	B	Exhaust	4	
12	3155236	B	Vent	2	
13	3169138	G	Amp	1	h = 0.016
14	3155018	E	Gasket	1	
15	3155040	G	Gasket	1	
16	3155021	B	Gasket	1	
17	3155021	F	Gasket	1	
18	3155216 M	D	Exhaust	2	Modified part
19	3155215	E	Exhaust	1	
20	3155213	D	Vent	3	
21	3155131	E	Amp	2	
22	3155213	D	Vent	3	
23	3155215	E	Exhaust	1	
24	3155216 M	D	Exhaust	2	Modified part
25	3155021	A	Gasket	1	
26	3155018	B	Gasket	1	
27	3155018	G	Gasket	1	
28	3155219	G	Nozzle	1	
29	3155217	E	Exhaust	1	
30	3155219	B	Nozzle	1	
31	3155217	D	Exhaust	1	
32	3155219	B	Nozzle	1	
33	3155040	D	Gasket	1	
34	3155040	G	Gasket	1	
35	3155018	G	Gasket	1	
36	3155020	A	Cap	4	
37	3155018	D	Gasket	1	
38	3155027	F	Resistor	4	
39	3155118	G	Transfer	2	
40	3155046	C	Gasket	1	
41	3155018	E	Gasket	1	
42	3155020	A	Cap	3	

AZIMUTH AXIS STACK NO. 2 (CONCLUDED)

Stack Sequence	Part Number	Orientation	Description	Quantity Required	Remarks
43	3155018	G	Gasket	1	
44	3155018	G	Gasket	1	
45	3155216 M	G	Exhaust	3	Modified part
46	3155237	B	Vent	1	
47	3155236	G	Vent	1	
48	3169138	B	Amp	1	h = 0.010
49	3155021	D	Gasket	1	
50	3155021	F	Gasket	1	
51	3155217	G	Exhaust	1	
52	3155021 M_1	B	Vent	3	Modified part
53	3155219	B	Nozzle	2	
54	3155018	E	Gasket	1	
55	3155216 M	D	Exhaust	3	Modified part
56	3155215	D	Exhaust	1	
57	3155213	D	Vent	3	
58	3155131	E	Amp	2	
59	3155213	E	Vent	2	
60	3155018	G	Gasket	1	
61	3155018	B	Gasket	1	
62	3155219	B	Nozzle	1	
63	3155217	E	Exhaust	1	
64	3155221	G	Nozzle	1	
65	3155216	B	Exhaust	1	
66	3155221	B	Nozzle	1	
67	3155217	D	Exhaust	1	
68	3155221	G	Nozzle	1	
69	3155216	B	Exhaust	1	
70	3155021	G	Gasket	1	
71	3155022	F	Gasket	1	
72	3155020 M	B	Exhaust	2	Modified part
73	3155000	G	Vent	2	
74	3155234	G	Amp	2	
75	3155000	B	Vent	2	
76	3155020 M	B	Exhaust	2	Modified part
77	3155018	E	Gasket	1	
78	3155021	D	Gasket	1	
79	3155027	A	Resistor	3	
80	3155018	G	Gasket	1	
81	3155191	G	Transfer	1	
82	3155018	B	Gasket	1	
83	3155191	B	Transfer	1	
84	3155019	A	Gasket	9	

ELEVATION AXIS STACK NO. 1

Stack Sequence	Part Number	Orientation	Description	Quantity Required	Remarks
1	3155033	A	Transfer	5	
2	3155047	G	Gasket	1	
3	3155062	H	Exhaust	4	
4	3155021	E	Gasket	1	
5	3155022	C	Gasket	1	
6	3155035	F	Transfer	3	
7	3155018	G	Gasket	1	
8	3155116	H	Transfer	3	
9	3155022	C	Gasket	1	
10	3155116	A	Transfer	3	
11	3155022	F	Gasket	1	
12	3155198	B	Exhaust	2	
13	3155237	B	Exhaust	2	
14	3155236	G	Vent	2	
15	3169138	B	Amp	1	h = 0.032
16	3155236	G	Vent	2	
17	3155237	B	Exhaust	2	
18	3155198	B	Exhaust	2	
19	3155021	C	Gasket	1	
20	3155219	E	Nozzle	2	
21	3155021 M_1	C	Vent	1	Modified part
22	3155219	E	Nozzle	2	
23	3155021 M_2	F	Gasket	1	Modified part
24	3155219	E	Nozzle	2	
25	3155021 M_2	A	Vent	1	
26	3155219	D	Nozzle	1	
27	3155021 M_2	C	Vent	1	
28	3155217	B	Exhaust	4	
29	3155019	A	Gasket	5	

ELEVATION AXIS STACK NO. 2

Stack Sequence	Part Number	Orientation	Description	Quantity Required	Remarks
1	3155033	E	Transfer	5	
2	3155217	G	Exhaust	4	
3	3155021 M_1	A	Vent	1	Modified part
4	3155219	H	Nozzle	2	
5	3155021 M_1	G	Vent	1	Modified part
6	3155219	C	Nozzle	2	
7	3155021 M_1	G	Vent	1	Modified part
8	3155219	C	Nozzle	2	
9	3155021 M_1	D	Vent	1	Modified part
10	3155219	C	Nozzle	2	
11	3155021 M_1	E	Vent	1	Modified part
12	3155219	H	Nozzle	2	
13	3155021 M_1	E	Vent	1	Modified part
14	3155219	H	Nozzle	3	
15	3155021 M_1	D	Vent	1	Modified part
16	3155219	C	Nozzle	3	
17	3155021 M_1	G	Vent	1	Modified part
18	3155219	H	Nozzle	2	
19	3155021 M_1	G	Vent	1	Modified part
20	3155219	H	Nozzle	3	
21	3155021 M_1	G	Vent	1	Modified part
22	3155219	C	Nozzle	2	
23	3155021 M_1	E	Vent	1	Modified part
24	3155219	C	Nozzle	2	
25	3155021 M_1	E	Vent	1	Modified part
26	3155219	H	Nozzle	2	
27	3155021 M_1	D	Vent	1	Modified part
28	3155219	G	Nozzle	2	
29	3155021 M_1	G	Vent	1	Modified part
30	3155219	C	Nozzle	2	
31	3155021	G	Vent	1	
32	3155219	C	Nozzle	2	
33	3155021	B	Vent	1	
34	3155219	H	Nozzle	2	
35	3155021 M_1	D	Vent	1	Modified part
36	3155219	C	Nozzle	2	
37	3155021 M_1	E	Vent	1	Modified part
38	3155219	H	Nozzle	3	
39	3155021	A	Gasket	1	
40	3155021	F	Gasket	1	

ELEVATION AXIS STACK NO. 2 (CONCLUDED)

Stack Sequence	Part Number	Orientation	Description	Quantity Required	Remarks
41	3155217	H	Exhaust	4	
42	3155021 M_1	C	Vent	2	Modified part
43	3155219	C	Nozzle	2	
44	3155021 M_1	G	Vent	1	Modified part
45	3155219	C	Nozzle	2	
46	3155021 M_1	G	Vent	1	Modified part
47	3155219	C	Nozzle	2	
48	3155021 M_1	B	Vent	1	Modified part
49	3155219	H	Nozzle	2	
50	3155021 M_1	D	Vent	1	Modified part
51	3155219	H	Nozzle	2	
52	3155021 M_1	G	Vent	1	Modified part
53	3155219	C	Nozzle	2	
54	3155021 M_1	D	Vent	1	Modified part
55	3155219	H	Nozzle	2	
56	3155022	G	Gasket	1	
57	3155198	F	Exhaust	2	
58	3155237	A	Exhaust	1	
59	3155236	A	Vent	2	
60	3169138	F	Amp	1	h = 0.030
61	3155236	A	Vent	2	
62	3155237	F	Exhaust	1	
63	3155198	F	Exhaust	2	
64	3155019	A	Gasket	5	

ELEVATION AXIS STACK NO. 3

Stack Sequence	Part Number	Orientation	Description	Quantity Required	Remarks
1	3155033	G	Transfer	3	
2	3155022	D	Gasket	1	
3	3155035	B	Transfer	3	
4	3155219	H	Nozzle	1	
5	3155040 M	D	Vent	1	Modified part
6	3155219	H	Nozzle	1	
7	3155021 M_1	H	Vent	1	Modified part
8	3155219	H	Nozzle	1	
9	3155040 M	A	Vent	1	Modified part
10	3155219	H	Nozzle	1	
11	3155040 M	D	Vent	1	Modified part
12	3155219	C	Nozzle	1	
13	3155040 M	D	Vent	1	Modified part
14	3155219	H	Nozzle	1	
15	3155040 M	E	Vent	1	Modified part
16	3155219	A	Nozzle	1	
17	3155040 M	D	Vent	1	Modified part
18	3155219	F	Nozzle	1	
19	3155217	C	Exhaust	1	
20	3155219	A	Nozzle	1	
21	3155040 M	D	Vent	1	Modified part
22	3155219	A	Nozzle	1	
23	3155022	E	Gasket	1	
24	3155021 M_1	H	Vent	1	Modified part
25	3155219	H	Nozzle	2	
26	3155021 M_1	E	Vent	1	Modified part
27	3155219	H	Nozzle	2	
28	3155217	A	Exhaust	2	
29	3155219	H	Nozzle	2	
30	3155021 M_1	E	Vent	1	Modified part
31	3155219	H	Nozzle	2	
32	3155021 M_1	G	Vent	1	Modified part
33	3155022	G	Gasket	1	
34	3155018	F	Gasket	1	
35	3155216 M	F	Exhaust	2	Modified part
36	3155237	H	Exhaust	1	
37	3155236	G	Vent	1	
38	3160138	C	Amp	1	h = 0.025
39	3155236	G	Vent	1	
40	3155237	H	Exhaust	1	

ELEVATION AXIS STACK NO. 3 (CONCLUDED)

Stack Sequence	Part Number	Orientation	Description	Quantity Required	Remarks
41	3155216 M	F	Exhaust	2	Modified part
42	3155018	H	Gasket	1	
43	3155018	C	Gasket	1	
44	3155018	H	Gasket	1	
45	3155198	F	Exhaust	2	
46	3155237	F	Exhaust	1	
47	3155236	A	Vent	1	
48	3169138	F	Amp	1	h = 0.020
49	3155236	A	Vent	1	
50	3155237	F	Exhaust	1	
51	3155198	A	Exhaust	2	
52	3155021	B	Gasket	1	
53	3155191	A	Transfer	2	
54	3155021	E	Gasket	1	
55	3155191	F	Transfer	3	
56	3155019	A	Gasket	5	

ELEVATION AXIS STACK NO. 4

Stack Sequence	Part Number	Orientation	Description	Quantity Required	Remarks
1	3155033	A	Transfer	4	
2	3155018	D	Gasket	1	
3	3155035	H	Transfer	3	
4	3155018	B	Gasket	1	
5	3155217	E	Exhaust	3	
6	3155021 M_2	E	Vent	1	Modified part
7	3155237	B	Exhaust	4	
8	3155236	G	Vent	2	
9	3169138	G	Amp	1	h = 0.016
10	3155018	E	Gasket	1	
11	3155040	F	Gasket	1	
12	3155217	E	Exhaust	1	
13	3155021 M_1	D	Vent	1	Modified part
14	3155219	E	Nozzle	1	
15	3155040 M	A	Vent	1	Modified part
16	3155219	E	Nozzle	1	
17	3155018	E	Gasket	1	
18	3155040	F	Gasket	1	
19	3155217	B	Exhaust	4	
20	3155021 M_2	G	Vent	1	Modified part
21	3155237	D	Exhaust	4	
22	3155236	E	Vent	2	
23	3169138	D	Amp	1	h = 0.010
24	3155018	B	Gasket	1	
25	3155018	B	Gasket	1	
26	3155011	A	Exhaust	2	
27	3155021	B	Gasket	1	
28	3155040	G	Gasket	1	
29	3155040	B	Gasket	1	
30	3155027	F	Cap	2	
31	3155018	E	Gasket	1	
32	3155027	C	Cap	3	
33	3155037	H	Transfer	2	
34	3155018	D	Gasket	1	
35	3155027	C	Cap	2	
36	3155018	G	Gasket	1	
37	3155040	B	Gasket	1	
38	3155040	C	Gasket	1	
39	3155217	B	Exhaust	1	
40	3155219	E	Nozzle	1	
41	3155040 M	H	Vent	1	Modified part

ELEVATION AXIS STACK NO. 4 (CONCLUDED)

Stack Sequence	Part Number		Orientation	Description	Quantity Required	Remarks
42	3155219		E	Nozzle	1	
43	3155021		E	Gasket	1	
44	3155216		G	Exhaust	3	
45	3155213		B	Vent	2	
46	3155131		G	Amp	2	
47	3155018		D	Gasket	1	
48	3155018		D	Gasket	1	
49	3155011		H	Exhaust	2	
50	3155021		D	Gasket	1	
51	3155024		B	Transfer	3	
52	3155018		G	Gasket	1	
53	3155021		A	Gasket	1	
54	3155020	M	B	Exhaust	2	Modified part
55	3155000		G	Vent	2	
56	3155234		G	Amp	2	
57	3155000		G	Vent	2	
58	3155020	M	B	Exhaust	2	Modified part
59	3155035		F	Transfer	3	
60	3155217		E	Exhaust	1	
61	3155219		G	Nozzle	1	
62	3155217		E	Exhaust	1	
63	3155219		G	Nozzle	1	
64	3155216		E	Exhaust	1	
65	3155219		G	Nozzle	1	
66	3155216		E	Exhaust	1	
67	3155019		A	Gasket	5	